Channel Allocation and post-CCA based Bandwidth Adaptation in Wireless Local Area Networks with Heterogeneous Bandwidths

Seowoo Jang

Ph.D. Dissertation

Abstract

The new prominent 802.11ac standard aims at achieving Gbps data throughput for individual users while at the same time guaranteeing backward compatibility. The approaches to achieving this goal use enhanced physical-layer features, such as higher modulation levels, MIMO (Multiple Input Multiple Output), and wider bandwidth. As for the bandwidth, the channel bonding technique that makes use of multiple 20MHz channels in 5GHz band is adopted. However, the heterogeneity of bandwidth in a network can cause asymmetric interferences in which some transmissions are not sensed by some nodes. As a result, the conventional CSMA/CA (Carrier Sense Multiple Access with Collision Avoidance) may not work well in 802.11ac networks and the Gbps throughput, which is attainable for a single link, is not achievable network-widely, which we call the *Hidden Channel* (HC) problem.

In this dissertation, we illustrate the *HC* problem with a 802.11ac network as a reference system. Then we analyze the problem using Markov chain technique and show how the contention parameters and

transmission time affect collision probability and fairness in some deployment scenarios. The validity of the analysis is verified through simulation in the same chapter.

As a solution to the *HC* problem, a centralized and heuristic channel allocation algorithm, *PCA* (Primary Channel Allocation), in an enterprise local area network is proposed in the next part of this dissertation. The *PCA* algorithm, a extended version of well known "University Timetabling" algorithm for incorporating multi-channel purpose, is designed to avoid *HC* problem effectively. Through simulations, we demonstrate that our proposed channel allocation algorithm lowers the packet error rate (PER) compared to uncoordinated and RSSI (Received Signal Strength Indicator) based allocation schemes and increases the network-wide throughput as well as the throughput of a station that experiences poor performance. This implies improved fairness performance among transmission pairs with various channel bandwidths.

Then, simple experiments are conducted with USRP and WARP boards to show that the problem is real and to prove that the validity of our next solution. Based on that, we argue for the need of bandwidth adaptation based on *post-CCA*, which is another clear channel assessment (CCA) procedure after finishing a transmission. The post-CCA helps mimic the CSMA/CD (CSMA with Collision Detection) mechanism in the wired Ethernet, thus enhancing channel assessment capability. Then, we propose *PoBA* (Post-CCA based

Bandwidth Adaptation) that alters bandwidth and channel configuration dynamically. Using simulation, we confirm that the PoBA increases network-wide throughput, channel utilization and fairness, and decreases packet error probability.

Keywords: channel allocation, post-CCA, bandwidth adaptation, asymmetric interference, hidden channel problem, heterogeneous bandwidth, local area network, HC, PCA, PoBA

Student Number: 2009-30931

Contents

1 Introduction **1**

1.1 Motivation 1

1.2 Contributions and Outline 6

2 The HC (Hidden Channel) Problem **11**

2.1 Introduction 11

2.2 Problem Description 15

2.3 Numerical Analysis 20

2.4 Simulation Results 27

2.5 Summary 31

3 PCA (Primary Channel Allocation) **33**

3.1 Introduction 33

3.2 Channel Allocation for Alleviating HC 39

3.2.1 Problem Formulation 43

3.2.2 A Heuristic Primary Channel Assignment Algorithm 51

3.3 Simulation Results 57
3.3.1 Case for a Network with Two APs 58
3.3.2 Case for a Chain Topology with Six APs 60
3.3.3 Case for Various Sized Random Networks . . . 62
3.4 Summary 68

4 PoBA (Post-CCA based Bandwidth Adaptation) 69
4.1 Introduction 69
4.2 Experimental Results 72
4.3 Post-CCA & PoBA 78
4.3.1 Post-CCA Operation 78
4.3.2 PoBA Algorithm 81
4.4 Simulation Results 89
4.4.1 Case for a Chain Topology with Six APs 90
4.4.2 Case for Various Sized Random Networks . . . 92
4.5 Summary 96

5 Conclusion 97
5.1 Research Contributions 97
5.2 Future Research Directions 99

List of Tables

2.7 Event outcome from states 26

3.1 802.11ac MCS levels and minimum receiver sensitivity (dBm). 35

3.2 Weight vectors. (Pair types are in MHz, C_M:Mutually reserving, C_T:Total invading, C_P:partial invading, C_B: mutually Blind, C_I: mutually Indifferent) 47

3.3 Notations used in the integer problem. 49

3.4 Channel allocation example of the heuristic algorithm. ($I = \infty$) 55

3.5 Channel allocation example of the RSSI based algorithm. 56

3.6 Tx. trial, error rate and throughput of each node in the 6-chain topology. Tx. (#), Err. (%) and Thr. (Mbps). 61

4.1 Post-CCA observations and intuitions. 78

4.2 Simulation results for the toy topology in terms of error rate (%), throughput (Mbps), and channel utilization (%) 91

List of Figures

2.1 Channelization of 802.11ac in USA. 12

2.2 Static and dynamic channel accesses in 802.11ac. . . . 13

2.3 Enhanced RTS/CTS in 802.11ac. 14

2.4 Hidden secondary channel collision problem where the allocated channel numbers on the left are from AP1's viewpoint. 16

2.5 Total and partial invading scenarios (downlink). 18

2.6 State space and transitions. The diagonal lines represent distinguishing line between two regions, and dots with arrow represent state transitions from one to another. Dots in 'F' region make transitions to one of the dots on the corresponding horizontal line, and those in 'S' region to one on the vertical line. If both transmits, then the next state can be any one on the entire space. 25

2.7 Collision rate and fairness performance vs. CW_{vic} (CW_{inv} = 32). 29

2.8 Collision probability vs. CW_{inv} ($CW_{vic} = 32$). 30

2.9 Collision probability vs. packet length ($CW_{vic} = 32$ and $CW_{inv} = 64$). 30

3.1 Channel reserving range vs. MCS level. 37

3.2 A victim pair (Tx. and Rx.) and an invader for PER calculation. 38

3.3 PERs of the total and partial invadings between 40MHz and 80MHz senders. x and y axes represent two dimensional coordinates in meters. 40

3.4 Channel index and configurations in the problem formulation. 44

3.5 Relations between primary channels allocated for neighboring APs. Each number inside a node and on an edge indicates the primary channel index and the channel relation between the primary channels of the two neighboring APs, respectively. 45

3.6 A heuristic approach for the vertex coloring. 51

3.7 An example of channel allocation for comparison. . . . 54

3.8 Empirical CDF of the victim's throughput according to the distance between the invader and the victim. . . 59

3.9 A chain topology and bandwidth allocation results. . . 60

3.10 Network-wide packet error rate, throughput and fairness performance in small sized networks. 63

3.11 Network-wide packet error rate, throughput and fairness performance in large sized networks. 65
3.12 CDF for PER when $N = 10$ and throughput increment ratio. 67

4.1 Ideal MCS levels on each bandwidth according to receiver sensitivity, where the number in a circle represents the MCS level and the x-axis is the required receiver sensitivity. 70
4.2 Power spectral density of full and half band transmissions. 74
4.3 Experimental topologies. 75
4.4 Experimental results for different topologies. 76
4.5 Post-CCA operation. 78
4.6 Action case studies according to bandwidth. 85
4.7 6-chain topology for simple simulation. 91
4.8 Simulation results with random topologies - error rate and throughput. 93
4.9 Simulation results with random topologies - utilization and fairness. 94

Chapter 1

Introduction

1.1 Motivation

Over the last decade, we have witnessed a dramatic increase of mobile data traffic due to the large-scale deployment of increasingly powerful mobile devices and the resulting proliferation of mobile applications. This trend is expected to continue in the foreseeable future [7, 5, 6]. To deal with this explosive growth of mobile traffic, there have been numerous efforts to increase wireless link/network capacity by developing new physical-layer technologies and/or improving the existing design. But these solutions are still unable to keep up with fast growing demands.

Bandwidth has been used in a static or fixed manner until recently. For example, 802.11a/b/g used one of 11 predefined channels, each with 20MHz bandwidth in 2.4GHz band. Also, even though 3GPP

LTE (Long Term Evolution) allows from 1.25MHz up to 20MHz, a system is required to choose one of the allowed bandwidths and a corresponding channel. However, the advance of hardware technology has made it possible to use wider bandwidth as defined in 802.11n and 802.11ac [9, 10] or dynamically change bandwidth according to the surrounding environments of a link as in [13, 14, 15, 16].

The wider and dynamically changing bandwidth introduces heterogeneous bandwidths into local area networks. 802.11n networks with up to 40MHz bandwidth will coexist with 802.11ac with up to 160MHz bandwidth in 5GHz band. Furthermore, LTE also enhances wireless capacity by exploiting bandwidth-related approaches [22, 23]. LTE-U (LTE in unlicensed band) is planning to make use of unlicensed spectrum at 5GHz band along with its cellular band. Thus, next-generation local area networks need to manage and handle problems caused by heterogeneous bandwidths to offer better user experiences.

Recently, the 802.11 Group has initiated the development of the next version, 802.11ax [8, 21]. As the name HEW (High Efficient WLANs) implies, its goal is to offer 4x enhanced user experience over the previous versions by improving WLAN to operate more efficiently. It includes not just enhancement of the physical-layer technology but also medium-access and network-layer technologies. The next-generation WLANs will be deployed in an environment where a large number of APs (Access Points) coexist to support higher throughput. In such an environment, it is more important to resolve medium-access

and network-layer conflicts. Therefore, the standardization group addresses the problems related to the medium access control and the network layer to make them operate more efficiently.

To be more systematically specific, the design goal of 802.11ac, the reference local area network system in this dissertation, is to offer very high throughput (VHT) and backward compatibility with legacy 802.11 specifications [9, 19]. The achievable throughput of 802.11ac is around 500Mbps on a single antenna station and could be greater than 1Gbps using multi-user MIMO (Multi-Input Multi-Output) techniques. Thus, this increase in capacity is expected to alleviate some of the traffic load that is being generated by these new devices.

A unique feature that differentiates 802.11ac from the legacy versions is its *channelization* i.e., *extended bandwidth*. 802.11ac allows a device to work on one of the 20MHz channels in 5GHz band to guarantee backward compatibility, however, it also allows bonding of multiple adjacent 20MHz channels to create an aggregate single channel when needed. In the standards of 802.11ac it is mandatory to support up to a single 80MHz channel, and optionally a simultaneous use of two separated 80MHz channels with channel aggregation technique or a single 160MHz channel.

In order to guarantee backward compatibility with legacy stations working only on a 20MHz channel, and compatibility among 802.11ac stations using different bandwidths, the contention method of 802.11n is also inherited. A 20MHz channel is used as a primary channel in

which ordinary backoff-based contention is performed. The remaining channels, called secondary channels, are sensed for a predetermined period to ascertain whether they are idle or not.

Detecting signals from multiple channels provides an additional challenge for which two different CCA (Clear Channel Assessment) levels are used in 802.11ac and 802.11n [17, 18, 19]. In 802.11n, the CCA sensitivity of the primary channel is -82dBm, which is used for decoding incoming packets, while that of the secondary channel is -62dBm that is used only for detecting the energy. This means that a device occupying a secondary channel of another device would be disadvantaged by 20dB when assessing channel idleness. In 802.11ac, the CCA sensitivity for the secondary channel is enhanced to -69dBm or -72dBm depending on the allocated bandwidth [19]. However, there is still a disparity between primary and secondary CCA sensitivities.

Another issue is that each station needs to use a fixed transmission power, regardless of its allocated bandwidth [9, 10]. Accordingly many recent dynamic bandwidth allocation systems [14, 15, 16] assume the fixed transmission power without considering RF (Radio frequency) front-end modification. This dissertation also assumes the fixed transmission power.

Because different stations may use different bandwidths with possibly some overlapping parts, the signal powers reaching each other can be different even under the same channel condition. Hence, the quality of the transmission could vary significantly causing unfairness.

Further, the fixed transmission power and the difference in CCA sensitivity and bandwidth usage lead to asymmetric sensing/reserving situations between two devices. This implies that a transmission from a device may not be sensed by another device while it is sensed in the other direction, so channel reservation is successful only in one direction. We call this problem the **Hidden Channel (HC)** problem throughput this dissertation. The HC problem has basically originated due to the heterogeneity of the channel and bandwidth usage. Our main goal in this dissertation is to develop solutions that alleviate the HC problem.

We use 802.11ac as a reference system and show that the conventional CSMA/CA may not work well in the upcoming local area communication networks with heterogeneous bandwidths. The *'Hidden Channel'* problem [11, 17, 18] is similar to the well-known 'hidden terminal' problem. The discordance of the physical locations between a transmitter assessing channel idleness and a receiver experiencing actual conflicts is a cause for the hidden terminal problem. As a solution to the problem, the RTS/CTS handshaking scheme resolves the spatial reserving disharmony by sending small control packets from the both sides. On the other hand, the hidden channel problem arises from discrepancy of bandwidth usage. Since the RTS/CTS messages themselves can suffer the hidden channel problem, the RTS/CTS scheme is not an adequate solution for it, Therefore, we need other means to resolve spectral reserving discrepancy.

1.2 Contributions and Outline

In this dissertation, we first briefly explore the 802.11ac contention mechanism. Then, we present the failure scenario of the conventional CSMA/CA in 802.11ac networks with heterogeneous bandwidths, the *hidden channel* problem, in the first part of the dissertation.

The hidden channel problem is then analyzed using Markov chain tools in a perpetrator - victim scenario. And how the contention parameters and the transmission time affect the error rate is presented with the analysis. Then, the validity of the analysis is verified using simulation.

In order to relax the assumptions used in the analysis for analytical tractability, packet error rate (PER) behaviors when the entire or some parts of the bandwidth are interfered are studied. The results are used in the rest of the dissertation when formulating a problem or running simulations.

Following that, The channel allocation problem with the hidden channel problem is modeled with the graph coloring and proven that it is NP-hard. As a first solution, *PCA*, i.e., primary channel allocation algorithm, which allocates the location of the primary channels of each APs, given the bandwidths, in an enterprise local area network, is proposed. The algorithm is heuristic since the hidden channel problem is NP-hard.

Using simulation we show that the *PCA* alleviates the hidden

channel problem, so the packet error rate decreases and the throughput of the entire network increases. The effect of the enhanced RTS/CTS proposed in the 802.11ac is also shown with the simulation results.

We also perform simple experiments with USRP [1] and WARP v.3 [2] to show that the problem is real. We show that the CCA result at one link is different from that of the other link depending on the physical locations and the bandwidths of neighboring links. In other words, one can sense the existence of the other transmission, but not vice versa. We then argue the need for the bandwidth adaptation and present the effect of the bandwidth selection.

As an another solution to the hidden channel problem, we propose a simple yet effective operation called 'post-CCA'. The post-CCA is letting the transmitting device assess the channel idleness of the entire channels that it has used once again after finishing a transmission. It helps the wireless system mimic the CSMA/CD operation in a wired Ethernet network. Finding out and knowing which channels or sub-channels are interrupted by other transmissions is important information to exploit.

With the post-CCA result, we propose *PoBA* (Post-CCA based Bandwidth Adaptation) that alters the bandwidth and the central frequency of a channel, to avoid the one-way interference. To the best of our knowledge, this is the first proposing the post-CCA in wireless networks and the corresponding bandwidth adaptation algorithm.

We also use simulation to show that the *PoBA* reduces the packet

error probability and increases the throughput in dense topologies compared to without it. Because handling the hidden channel problem makes some links suffer from the always-intruding interference free from interruption, the *PoBA* also increases the fairness of the network. The results are consistent with the design philosophy of the next-generation WLAN, 802.11ax, that aims to increase actual user experience from the perspective of network design.

The following are the summary of the key contributions of our dissertation.

- We present the *Hidden Channel* problem that arises due to the heterogeneity of the bandwidth in the local area networks.
- We analyze the hidden channel problem, or the asymmetric channel sensing/reserving situation, from the perspective of downlink communication, and illustrate via numerical results how the contention parameters and the packet length impact performance.
- We use graph coloring to model the channel allocation problem, and prove that the problem is NP-hard.
- We present a heuristic algorithm that aims to eliminate the HC problem while maximizing channel utilization.
- We evaluate the performance of our heuristic algorithm with simulations. To the best of our knowledge, this is the first work

that explicitly deals with channel allocation to alleviate the HC problem in 802.11ac networks.

- Then, we conduct simple experiments with USRP [1] and WARP v.3 [2] to confirm that the HC problem is real in actual environments.

- We propose a simple yet effective operation called *'post-CCA'* that senses the channel idleness once again after completing a transmission. Finding out and knowing which channels or subchannels are interrupted by other transmissions is important information to exploit.

- We then propose *'PoBA'* that changes bandwidth and channel configurations dynamically to avoid the one-way interference by using the post-CCA operation in a distributed manner. To the best of our knowledge, this is the first work that proposes post-CCA operation in wireless systems and corresponding bandwidth adaptation.

- We evaluate the performance of PoBA using simulation. The PoBA relieves the packet error rate by 25% and increases the throughput more than 50% compared to without it on average in a dense network.

The rest of the dissertation is organized as follows. In Chapter 2, we present the hidden channel problem in 802.11ac systems and show

the analysis and experiments in detail. Then, in Chapter 3, the graph coloring model of the channel allocation problem is presented. And the first solution *PCA*, primary channel allocation algorithm, is proposed in the same chapter. In Chapter 4 we first conduct simple experiments to show that the problem is real and to prove the validity of our next solution. Then, the post-CCA operation is proposed with the PoBA algorithm as the second solution to the problem. We finally conclude the dissertation in Chapter 5 with the summary of contributions and future works.

Chapter 2

The HC (Hidden Channel) Problem

2.1 Introduction

In this chapter, we briefly introduce the new features of 802.11ac designed for throughput enhancing purpose. Then the *HC* (Hidden Channel) problem is detailed. The problem in a simple perpetrator, i.e., invader and a victim is then analyzed with Markov chain, and the simulation results regarding the problem situation are presented.

As briefly mentioned in the previous chapter, 802.11ac allows APs to only use non-overlapping channels, as illustrated in Fig. 2.1[9, 19]. This concept is inherited from the design philosophy of 802.11n, which tries to avoid in-band interference in a simple manner. Two adjacent 20MHz channels form a 40MHz channel, and two adjacent 40MHz

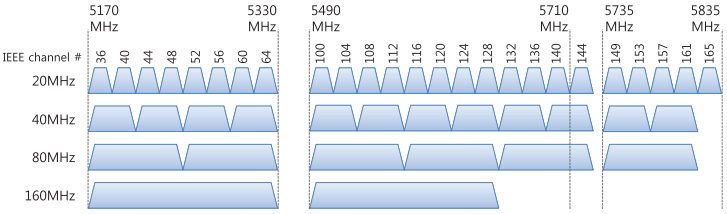

Figure 2.1: Channelization of 802.11ac in USA.

channels an 80MHz channel. A 160MHz channel can be formed either by merging two adjacent or separated 80MHz channels with channel aggregating technique.

The contention scheme in 802.11ac is characterized by a primary channel separated from secondary channels. To support this expanded channelization (by differentiating between primary and secondary channels), each AP uses control fields in the beacon to indicate its bandwidth and primary channel number [9].

Also, 802.11ac defines two different CCA sensitivities for the primary and secondary channels. In the case of 20MHz and 40MHz bandwidths, the primary channel sensitivities are -82dBm and -79dBm, respectively, while the secondary sensitivity for the both bandwidths is -72dBm. The primary and secondary sensitivities for 80MHz bandwidth are -76dBm and -69dBm, respectively [9]. The primary sensitivity is for decoding incoming packets, while the secondary sensitivity for detecting energy density. So, depending on the channel configurations between neighboring devices, there can be a discrepancy in the sensing/reserving capability among them as follows.

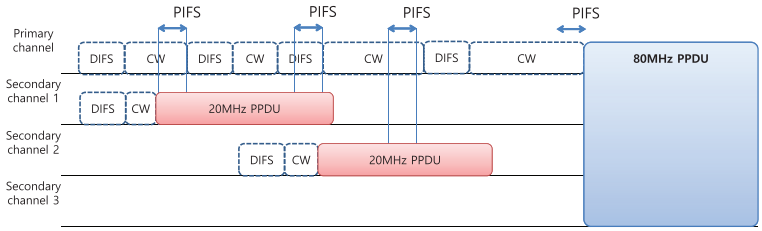

(a) Static access

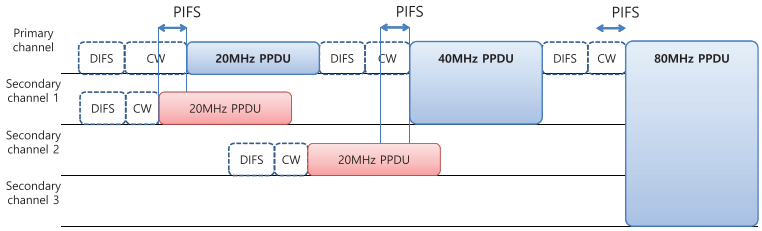

(b) Dynamic access

Figure 2.2: Static and dynamic channel accesses in 802.11ac.

For the primary channel, each station uses the legacy contention method. After the DIFS (DCF Inter-Frame Spacing) period, it selects a backoff counter and waits for the backoff counter to reach zero. Before the counter expires, however, the station senses secondary channels for one PCF Inter-Frame Spacing (PIFS) period. When all the primary and secondary channels are idle, the station starts transmitting. However, if not all the secondary channels are idle, the station has two choices as shown in Fig. 2.2; static access and dynamic access[9, 17, 18, 19]. In static access, the station retries to access the entire channel by choosing a new random backoff counter. In dynamic access, the station transmits over the primary channel and only the idle secondary channels that are adjacent to the primary one, exclud-

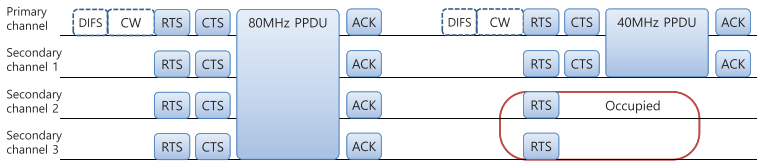

Figure 2.3: Enhanced RTS/CTS in 802.11ac.

ing busy secondary channels. Static access is mandatory, while the dynamic access is optional. In this dissertation, we only focus on static access.

Optionally, the enhanced RTS/CTS scheme can be used for spatial reserving in 802.11ac [9, 17, 19]. In this scheme, a transmitter sends RTS (Request-to-send) to a receiver before attempting a transmission. The RTS message is in the format of 802.11a RTS frame for backward compatibility, and thus occupies only 20MHz. To reserve the entire channel, 802.11a RTS frames are duplicated for each 20MHz channel as in Fig. 2.3. The receiver checks the idleness of each channel upon receiving the RTS frame, then sends back a CTS (Clear-to-send) message after SIFS (Short Inter-Frame Spacing) duration on each idle channel. Other nodes receiving either RTS or CTS frame, regard corresponding channels busy and defer their transmissions for the NAV (Network Allocation Vector) durations specified in the RTS/CTS frames. The enhanced RTS/CTS can be used along with the dynamic access shown on the right side of Fig. 2.3.

The new features above in heterogeneous bandwidth network cause the asymmetric channel sensing/reserving situation, i.e., the *hidden*

channel problem detailed as follows.

2.2 Problem Description

As mentioned before, a collision could occur because the CCA levels for the primary and secondary channels are different [17, 18, 19], and such a collision is called the hidden secondary channel (HSC) problem. (The hidden secondary channel problem is a subset of the HC problem, which will be addressed later.) Fig. 2.4 illustrates an example of the HSC problem between AP1 of an 80MHz channel and AP2 of a 20MHz channel. This type of collision happens when the two APs are within the primary channel sensing range but out of the secondary channel sensing range. AP1 cannot sense a PPDU (Physical layer Protocol Data Unit) transmission from AP2 which occupies one of the three secondary channels of AP1 because its received PPDU power lies between the primary and secondary CCA levels. So, after contending on its primary channel and believing that the secondary channels as idle, AP1 transmits its PPDU even while AP2 is transmitting.

In this chapter, we call the sender, whose transmission is corrupted due to this asymmetry, the 'victim', and the other sender that "invades" the victim's transmission, an 'invader'. In Fig. 2.4, AP1 is an invader while AP2 is a victim.

In the HSC problem scenario described so far, invading occurs from an AP using larger bandwidth to another using smaller bandwidth.

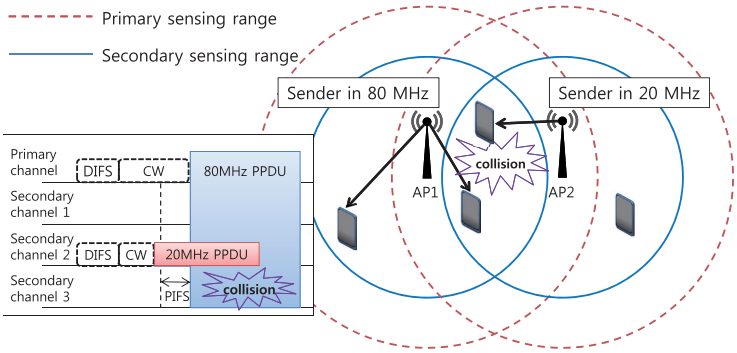

Figure 2.4: Hidden secondary channel collision problem where the allocated channel numbers on the left are from AP1's viewpoint.

The invading happens when the smaller bandwidth consists of only secondary channels of the larger bandwidth, causing an asymmetric sensing/reserving situation.

However, due to the fixed transmission power of an AP, regardless of the allocated bandwidth, the invading direction represents a mutual relation between the two APs that use larger bandwidth and smaller bandwidth, respectively. When an AP sends packets in a 20MHz channel, the full transmission power, for example, 17dBm is concentrated on the single 20MHz bandwidth. If it exploits 40MHz channel, it distributes 17dBm power over 40MHz, so its transmission power per 20MHz is reduced by half (i.e. 14dBm). In this manner, an AP exploiting 80MHz and 160MHz gets 11dBm and 9dBm, respectively. In other words, power density decreases with the bandwidth. Since the channel sensing is performed per 20MHz channel, the different power level injected per 20MHz channels can affect the result

of the channel assessment.

For better understanding, we use the notion of "reserving range" instead of sensing range from now on. The results of channel sensing on both primary and secondary channels depend on the CCA sensitivities and transmission powers of other transmitting nodes. From this perspective, there are two types of reserving range depending on the type of the channel on which the channel reservation is performed. The primary reserving range of a node is the distance within which some other nodes can sense its transmission over their primary channels with the primary CCA threshold. Likewise, secondary reserving range is that with the secondary CCA threshold. Both reserving ranges are defined from the viewpoint of a sender to make other nodes give up their transmissions.

On the other hand, the sensing range of a node is the distance within which an AP can sense some other node's transmission. It is defined from the perspective of the sensing node. Reserving range and sensing range are complementary and their main difference comes from which perspective, is the range is defined.

Fig. 2.5 illustrates two invading scenarios with different choices of bandwidths and primary channels. In the figure, the primary reserving ranges are represented with dotted circles and the secondary reserving ranges with solid circles. Bandwidth and primary channel choices are shown on the left. Filled squares represent primary channels, shaded squares secondary channels, and empty squares unused

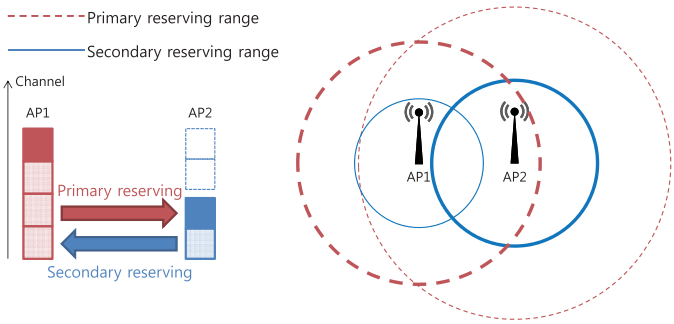

(a) Total (bandwidth) invading

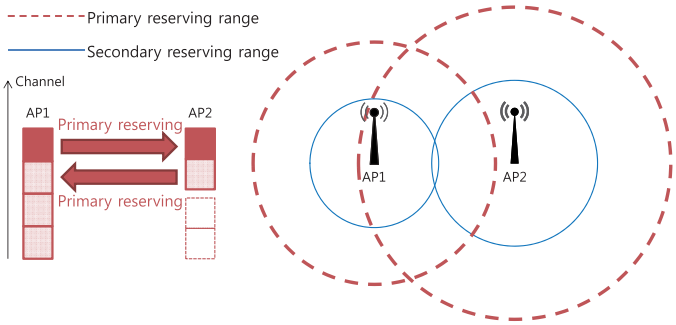

(b) Partial (Bandwidth) invading

Figure 2.5: Total and partial invading scenarios (downlink).

channels. AP1 and AP2 use 80MHz and 40MHz channels, respectively. Since AP1 consumes a weaker power per 20MHz than AP2, the reserving range of AP1 is smaller than that of AP2.

In Fig. 2.5(a), AP1 chooses the first 20MHz channel as its primary channel while AP2 chooses the third channel as its primary channel. When AP1 transmits, its transmission can be sensed by the primary CCA sensitivity of AP2. So AP1 is 'primary reserving'. If AP2 transmits, its transmission is only sensed by the secondary CCA

sensitivity of AP1. Thus, AP2 is 'secondary reserving'. Upon observing the primary reserving range of AP1 and the secondary reserving range of AP2, we find that the former is longer and covers AP2 while the latter does not cover AP1. Therefore AP1 reserves the channel successfully but AP2 does not. We call this case 'Total (bandwidth) Invading' because one using a larger bandwidth invades one using a smaller bandwidth over the entire bandwidth. This case is the same as HSC problem.[1]

In Fig. 2.5(b), we show a different scenario. Both APs choose the first 20MHz channel as their primary channel. In this case, they can sense each other with the primary CCA sensitivity. However, AP1's power per 20MHz channel is weaker than AP2's. So, the primary reserving range of AP1 is shorter than that of AP2. When they are located somewhere in the middle of their reserving ranges, AP1 fails in channel reserving while AP2 succeeds. We name this case 'Partial (bandwidth) Invading' in which a smaller bandwidth AP invades a larger bandwidth one in some band.

These two invading scenarios are considered as the HC Problem because the whole or a part of channels that some other node uses are not sensed properly. Therefore an invading AP transmits while some other node(s) is transmitting. Furthermore, depending on the relative location of each node, some APs always get invaded, which results in poor fairness performance.

[1]We use the term 'total invading' instead of HSC from now on.

For MAC, an enhanced RTS/CTS handshake scheme can be adopted to ease the total invading problem [17]. However, it cannot solve it properly because it does not consider the sensing asymmetry. To be more specific, the RTS/CTS scheme aims to reserve space by transmitting small sized control packets on both transmitter and receiver sides. The RTS/CTS frames also suffer the invading problem since they are transmitted over the entire bandwidth with the fixed transmission power. We evaluate the effectiveness of the enhanced RTS/CTS on the problem in Chapter 3.

In the next chapter, we take an approach to managing the primary channel allocation to eliminate the HC Problem while maximizing the channel utilization. To the best of our knowledge, this is the first work that considers the sensing asymmetry in 802.11ac networks so far. Before describing the channel allocation scheme, we first provide a methodology to analyze a specific scenario with a Markov chain, then show that the analysis results match with simulation results.

2.3 Numerical Analysis

To understand the effect of 802.11 backoff-based MAC (Medium Access Control) in the problem situation, we analyze a simple invading scenario using a discrete time Markov chain model. The considered scenario is shown in Fig. 2.4 where a pair of victim and invader suffer from the HC problem. For analytical tractability, we assume that

collision happens when the transmissions of the two senders overlap in time, and the contention window size is fixed, i.e., no binary exponential backoff. We also assume that the transmission time is fixed for both pairs.

The state of the chain is defined as a tuple of two integers, (i, v), each representing the selected backoff counters for the invader and the victim, respectively. Each state leads to an outcome which indicates whether or not the invader and the victim attempt to transmit and their transmissions are successful. Along with contention collision, in which two senders start to transmit at the same time, there are five possible outcomes. Then the state transition occurs according to the new random counter and the amount of time corresponding to the outcome. With transition probabilities, we can derive the steady state probability of each state by solving a homogeneous linear system. By adding the probabilities of all the states that lead to a same outcome, we can calculate the attempt and collision rates of the invader and the victim.

In the model, a state transition happens when either one of the senders enters a backoff stage. Each state is represented by a random backoff counter pair (i, v) of the invader and the victim. Assume for the time being that the contention window size (CW) is fixed at 32, and the packet transmission time is also fixed. The random counter value decides whether the transmission is successful or not. For example, if $(i, v) = (8, 20)$ and both can sense each other, the

victim will freeze its counter when the invader starts transmission after 8 backoff slots. Then the next state becomes $(newcounter, 20 - 8)$.

However, in an HC problem situation, it gets complicated. For $v > i$, the victim freezes and the invader will have a new random counter after having a successful transmission. So the newly selected counter and $(v - i)$ will form a next state. Since the new random counter is uniformly distributed within CW, the transition probability from (i, v) to $(newcounter, v - i)$ will be uniformly distributed on the $(v - i)$ line of the victim counter. This is the same as the symmetric scenario and denoted by 'F' (frozen) in Fig. 2.6.

In contrast, for $v < i$, the victim will start transmission first after waiting v slots. Unfortunately, the invader will also transmit after i slots, because it cannot sense the victim's transmission. Depending on the difference of the counter values, there are three possible cases.

1. If the counter difference is smaller than the victim's transmission time, a collision occurs, denoted by 'C' in Fig. 2.6. After the collision, both select new random counters. Collision occurs again if both happen to have a same random counter, denoted by 'CC' (Contention Collision) in the figure.

2. If the difference is greater than the victim's transmission time and smaller than the transmission time plus DIFS, the invader comes into the medium after the victim finishes transmission but before the victim enters a backoff stage. In this case, the

victim and the invader sequentially succeed in their transmissions, denoted by 'SS' (Sequentially Success) in the figure, and the next competition with new counters begins after the invader ends its transmission.

3. If the difference is greater than the victim's transmission time plus DIFS, the victim finishes its transmission successfully and enters a new backoff stage after DIFS. The next state is randomly chosen on the line of *invader counter* = *n-m-l-d*, denoted as 'S' in the figure. Here, l is the victim's packet transmission time, and d is DIFS which is given as 4 slots from the 802.11 specification.

The Markov chain model for the above can be expressed as follows.

$$\begin{bmatrix} s_1 \\ \vdots \\ s_K \end{bmatrix} = \begin{bmatrix} p_{1\leftarrow 1} & \cdots & p_{1\leftarrow K} \\ \vdots & \ddots & \vdots \\ p_{K\leftarrow 1} & \cdots & p_{K\leftarrow K} \end{bmatrix} \times \begin{bmatrix} s_1 \\ \vdots \\ s_K \end{bmatrix} \tag{2.1}$$

$$\sum_{i=1}^{K} s_i = 1 \tag{2.2}$$

$$\sum_{i=1}^{K} p_{i\leftarrow j} = 1 \tag{2.3}$$

Here K is the total number of states, which equals the multiplication of the contention windows of the victim and the invader. The steady state probability of state i is expressed as s_i, and $p_{i\leftarrow j}$

represents the state transition probability from states j to i. Eqs. 2.2 and 2.3 indicate that the sums of all the state probabilities and all the outgoing transition probabilities from state j are unity, respectively.

There exists a unique solution if the rank of the transition matrix equals the number of unknown variables, s_i. From Eq. 2.3, the rank of the transition probability matrix is $K-1$. Using Eq. 2.2, we obtain

$$\begin{bmatrix} \mathbf{I}-\mathbf{P} \\ \mathbf{1} \end{bmatrix} \times \mathbf{S} = \mathbf{0}, \tag{2.4}$$

where $\mathbf{P}$ is the transition probability matrix, $\mathbf{I}$ is the identity matrix, $\mathbf{1}$ is the raw vector in which all the elements are one, and $\mathbf{S}$ is the steady state probability matrix. By solving this homogeneous linear system, we can obtain a unique solution since the rank of the coefficient matrix is K. Then we obtain the steady state probability for each type of F, C, CC, S and SS by adding all the state probabilities of each area.

For simplicity, we use the mapping table in Table 2.7, which summarizes the outcomes from each category of states. Each element of the outcome vector indicates whether the invader transmits ('1'), the invader's packet is corrupted ('1'), the victim transmits ('1'), and the victim's packet is corrupted ('1'), or otherwise ('0'), respectively. For type F, the invader successfully transmits while the victim freezes. So we can express the outcome vector as $(1, 0, 0, 0)$. For type C, the outcome is $(1, 1, 1, 1)$ which indicates that both transmit and collide. As

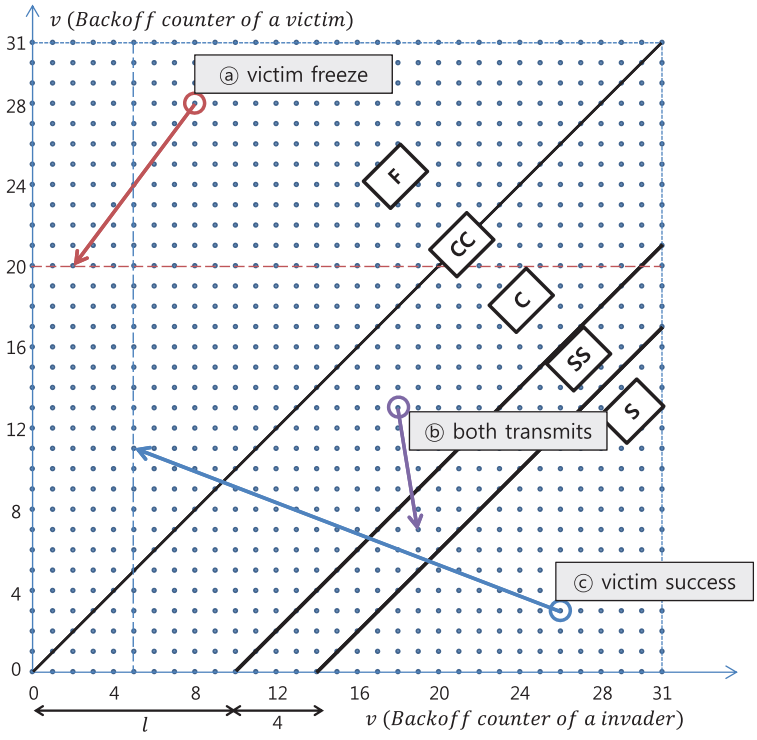

Figure 2.6: State space and transitions. The diagonal lines represent distinguishing line between two regions, and dots with arrow represent state transitions from one to another. Dots in 'F' region make transitions to one of the dots on the corresponding horizontal line, and those in 'S' region to one on the vertical line. If both transmits, then the next state can be any one on the entire space.

Table 2.7: Event outcome from states

State type	**Event Outcome**
F (frozen)	(1, 0, 0, 0)
C (Collision)	(1, 1, 1, 1)
CC (Contention Collision)	(1, 1, 1, 1)
S (Success)	(0, 0, 1, 0)
SS (Success & Success)	(1, 0, 1, 0)

collision occurs during their packet transmissions, they do not necessarily have the same backoff time. For type CC, the collision happens during the contention resolution, resulting in the same outcome as type C. For type SS, both transmit successfully in sequence, so the outcome is $(1, 0, 1, 0)$. And for type S, only the victim transmits and the state is expressed as $(0, 0, 1, 0)$.

Calculating the collision probabilities is now straightforward. The victim transmits in state C, CC, S and SS. And it experiences collision in C and CC. So the victim's collision probability can be calculated by separating the collision probability from the transmission probability. Likewise, the invader's collision probability can be obtained from separating the probabilities of C and CC from those of F, C, CC and SS. We can also derive the fairness performance of the two senders in the sense of their transmission attempts in the same way.

The analysis can be extended to derive other types of relations between the two senders by using different assumptions for collision, error model, and contention window size. For example, an extension that allows different contention window sizes is possible by adding

more states. In 802.11, the basic contention window size is 32 and doubles up to 1024 whenever a transmission failure occurs. In this case, the state space can be extended in x and y axes according to the contention window sizes of the invader and the victim, respectively.

However the lines that distinguish between F, C, CC, S, and SS regions remain the same unless the packet transmission time of the victim varies. If the transmission time changes, the two lines distinguishing between C, SS, and S will be shifted by the amount of transmission time.

2.4 Simulation Results

We now show the collision probability and attempt-fairness in the invading scenario through the results of the Markov analysis and simulations. Fig. 2.7 shows the numerical and simulation results for the collision probability when the invader uses the fixed CW_{inv} of 32 and the victim has varying CW_{vic}. The simulation time is 1 second with saturated traffic. Two APs are appropriately separated to suffer the invading according to the following channel model.

$$PL(d) = 20 \cdot log(\frac{4\pi d_0}{\lambda}) + 10n \cdot log(\frac{d}{d_0}). \tag{2.5}$$

Here n is the path loss exponent and set to 3, d is the distance between transmitter and receiver where d_0 is the reference distance which is set to 1m in our simulations, λ is the wavelength of 5.3GHz.

And we use the transmission power of 17dBm. This channel model will be used throughout this dissertation.

As shown in the graph, the numerical results match well with the simulation results. The collision probability of the victim in Fig. 2.7(a) is nearly 50% for all CW_{vic} and that of the invader stays below 3%. As expected, the collision probability of the victim does not decrease with CW_{vic}. This is because the invader is insensitive to the victim's transmission. Fig. 2.7(b) shows that increasing the victim's contention window size only lowers its transmission attempt rate. It can be seen that the transmission attempt of the victim normalized by that of the invader decreases with CW_{vic}.

To make the transmission opportunity fair, one can set the CW_{inv} larger than the CW_{vic}. This allows more time for the victim to finish its transmission before the invader comes in as shown in Fig. 2.8. The victim uses the fixed CW_{vic} of 32 and the invader varies CW_{inv}. As shown in the graph, the collision probability of the victim decreases with CW_{inv}. However the decrement in collision probability is highly dependent on the packet transmission time. The collision probability versus packet length is shown in Fig. 2.9.

The collision probability of the invader barely varies and stays below 3% under all circumstances while that of the victim is around 50% and fluctuates heavily depending on contention parameters. Therefore, we can say that the 802.11 contention resolution scheme does not handle the channel asymmetry effectively.

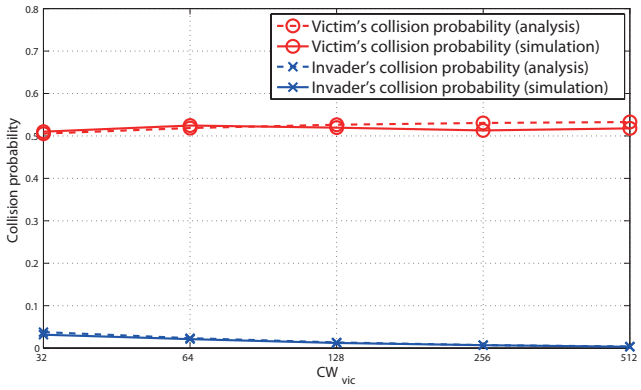

(a) Collision rate of invader and victim

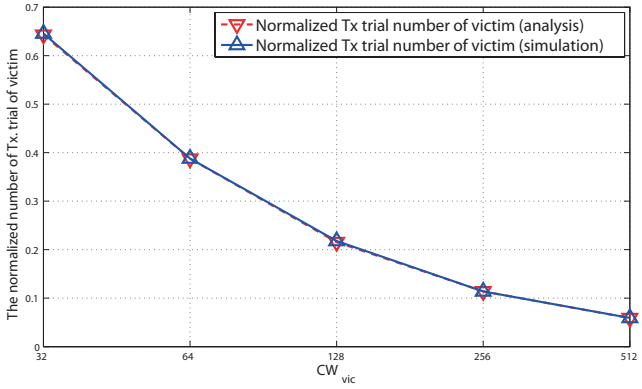

(b) Fairness performance of invader and victim

Figure 2.7: Collision rate and fairness performance vs. CW_{vic} (CW_{inv} = 32).

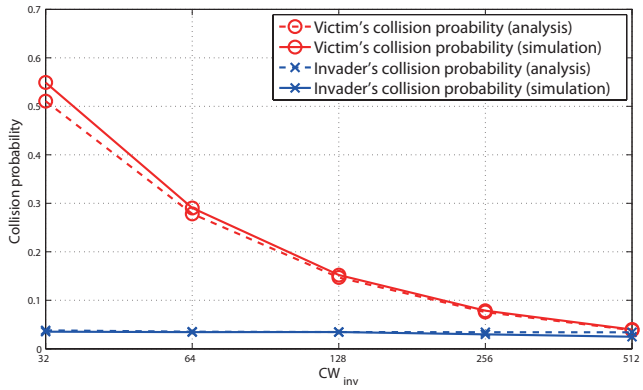

Figure 2.8: Collision probability vs. CW_{inv} ($CW_{vic} = 32$).

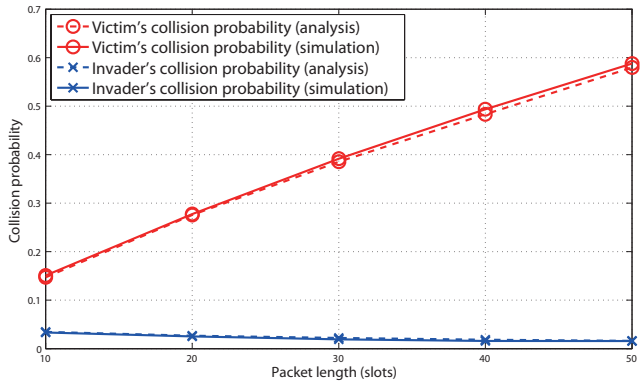

Figure 2.9: Collision probability vs. packet length ($CW_{vic} = 32$ and $CW_{inv} = 64$).

One could design a contention window managing scheme that aims to reduce the collision probability of the victim. However, this approach requires lots of information and a huge overhead for exchanging the information among transmission pairs or to/from APC. Further, tracking an optimal size of contention window is difficult when the assumptions made in this section do not hold, i.e., topology, collision and backoff assumptions. We leave this approach as a future work.

So our approach aims to alleviate the problem by channel allocation, which tries to make the invader and the victim contend as fair as possible, while maximizing bandwidth utilization.

2.5 Summary

In this chapter, the 802.11ac channelization and contention mechanism are briefly explored. Then, we presented the *HC* problem that arises in 802.11ac networks with heterogeneous bandwidth. The problem is analyzed with discrete Markov chain and the validity of the analysis is verified using simulation. Through the analysis and simulation, it is confirmed that the contention parameters, contention counters of the victim and the invader, affect the packet error rate severely. Also the relative packet transmission time is shown to be another factor that influence the performance.

The analysis and simulation in this chapter assume the impractical condition, time overlapping error event. In the following chapter, we

first break the assumption by exploring how to set the error event more, then formulate the channel allocation problem and propose the primary channel allocation algorithm.

Chapter 3

PCA (Primary Channel Allocation)

3.1 Introduction

In this chapter, packet error behaviors when the entire or parts of the channel are interfered by other transmission is firstly presented. The PER behavior will be used in the following sections and chapters. Then we formulate primary channel allocation problem with graph coloring and show that the problem is NP-hard. Following that, the primary channel allocation (PCA) algorithm to alleviate the hidden channel problem is proposed and explained in detail. The performance of the PCA scheme in simple and random topologies with and without the enhanced RTS/CTS scheme is shown using simulation.

While the above analysis, provides some intuition and understand-

ing of the impact of various parameters on performance, the actual packet reception performance is affected by various factors, and SINR (Signal to Interference & Noise Ratio) is one of those. When two packets collide, the SINR of the desired packet at a specific receiver can be sufficiently high enough. In this case, the receiver is enabled to decode the received packet successfully. This phenomenon is called the capture effect [38].

Another factor that affects the packet reception performance is an AMC (Adaptive Modulation and Coding) scheme which adaptively switches modulation and coding according to the channel condition. IEEE 802.11ac uses 10 MCS (Modulation and Coding Scheme) levels including 256-QAM (Quadrature Amplitude Modulation) with 5/6 redundancy [9].

In this section, we first consider the relations between MCS levels, the distance between a transmitter and a receiver, and primary/secondary reserving ranges. Then the numerical results for PER performance when the HC problem exists are presented. Briefly speaking, even under a perfect AMC scheme, the PER of a victim receiver increases due to the interruption of the invader. The PER will be used as a performance metric in Section 3.3.

With the receiver sensitivity (RS)[1] and the channel model of Eq. 2.5, we can obtain the maximum distance that a packet with a specific MCS level can be delivered successfully. Table 3.1 summarizes MCS

[1]It is the minimum received signal power required for decoding the signal with the error probability of smaller than 10%.

Table 3.1: 802.11ac MCS levels and minimum receiver sensitivity (dBm).

MCS index	Mod.	Cod.	20MHz	40MHz	80MHz	160MHz
0	BPSK	1/2	-82	-79	-76	-73
1	QPSK	1/2	-79	-76	-73	-70
2	QPSK	3/4	-77	-74	-71	-68
3	16-QAM	1/2	-74	-71	-68	-65
4	16-QAM	3/4	-70	-67	-64	-61
5	64-QAM	2/3	-66	-63	-60	-57
6	64-QAM	3/4	-65	-62	-59	-56
7	64-QAM	5/6	-64	-61	-58	-55
8	256-QAM	3/4	-59	-56	-53	-50
9	256-QAM	5/6	-57	-54	-51	-48

levels supported in channels with the required minimum RS. The maximum reserving ranges are achievable with the CCA thresholds for the primary and secondary channels, which are -82dBm and -72dBm, respectively [19].

Fig. 3.1 shows the maximum distance and data rate for each MCS level with primary/secondary reserving ranges of 40MHz and 80MHz transmissions calculated from Table 3.1.[2] Due to the decreased transmission power per 20MHz, the reserving range decreases with increasing channel bandwidth. The maximum distance for each MCS level decreases due to the increased RS. In general, wider bandwidth and higher RS lead to increased data rates at the cost of reduced trans-

[2]The numerical results of reserving ranges for 20MHz and 160MHz channels are not presented due to the page limit. However, they show the same tendency of having decreased reserving range and increased data rate with the bandwidth size.

mission and reserving ranges.

If a 40MHz transmitter is 25m apart from an 80MHz transmitter and their channel settings are the same as in Fig. 2.5(a), the 80MHz one becomes the invader and the 40MHz one becomes the victim because the primary reserving range of the 80MHz one is 34m while the secondary reserving range of the 40MHz one is 20m (Total Invading). On the other hand, if they are located 40m apart with the channel configuration as in Fig. 2.5(b), the 40MHz one invades the 80MHz one because the primary reserving ranges of the former and the latter are 43m and 34m, respectively (Partial Invading).

We now calculate the PERs for the total and partial invadings between the 40MHz and 80MHz transmissions. Fig. 3.2 shows a scenario used for the numerical calculation of PER. There is a victim pair (d[m] apart) and an invading sender that interrupts transmission of the victim pair. Here, the victim sender is located at zero coordinates, and the victim receiver's location varies. And the invader is located D[m] apart from the victim sender. The invader is set to suffer the HC problem, and d and θ vary within reachability. Assuming P_{tx} and P_{rx} represent the transmission powers of the victim sender and the invader, respectively, in a single 20MHz channel, the SIR (Signal to Interference Ratio) at the victim receiver can be calculated from the following equation.

$$SIR = \left(\frac{D^2 + d^2 - 2dDcos\theta}{d^2}\right)^{\frac{n}{2}} \times \frac{P_{tx}}{P_{rx}} \tag{3.1}$$

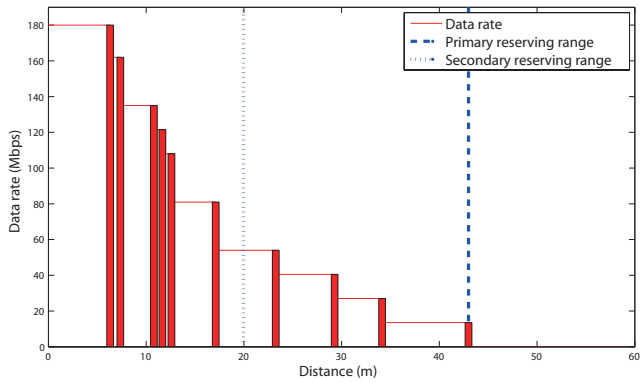

(a) Ranges in 40MHz channel

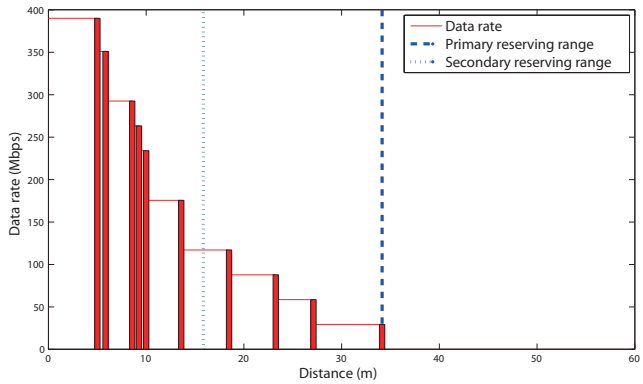

(b) Ranges in 80MHz channel

Figure 3.1: Channel reserving range vs. MCS level.

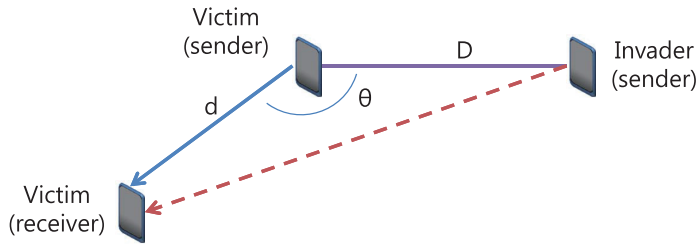

Figure 3.2: A victim pair (Tx. and Rx.) and an invader for PER calculation.

The difference in the channel bandwidths that the victim and the invader are exploiting is considered so that the error rates of all the 20MHz channels are averaged to obtain the effective PER. Then the effective SINR of the entire channel can be derived reversely. The way of calculating the effective PER and the SINR is the same as in [24] except that they calculate the PER as an average over all available subcarriers instead of channels. While calculating the PER from the SINR, we adopt the PER equation in [20] because it is effective in incorporating various MAC layer operations such as perfect AMC scheme, Viterbi algorithm, and packet size (1500bytes in our case).

Fig. 3.3 shows the PER performances of the total and partial invadings between 40MHz and 80MHz senders. Recall that the one with larger bandwidth invades smaller one in total invading, and vice versa in partial invading. Here, dark (red) and gray (green) colors represent the PERs of 1 and 0, respectively. In Fig. 3.3(a) and 3.3(b), the invader is located at $(25, 0)$ and $(40, 0)$, respectively. The sender

of the victim pair is located at the origin while its receiver spans the transmission range of the sender. It can be seen that the maximum transmission distance of 80MHz one is shorter than that of 40MHz one. The average PERs in the total and partial invadings are 83% and 32%, respectively. This shows that using wider bandwidth results in lower PER due to the reduced transmission range.

The numerical results show impact of invading in terms of PER for both directions. One using a larger bandwidth tends to be an invader when separated by a shorter distance while the one using a smaller bandwidth over a longer distance. The PER can be incorporated into the outcome of each event in the Markovian analysis presented in the appendix. And from now on, as a performance metric, we use the PER instead of 'collision probability'.

3.2 Channel Allocation for Alleviating HC

In this section, we formulate the channel allocation problem using graph theory. We assume that the interference map among APs is known a priori. The interference relation among APs is assumed to be derived from the aggregated AP information reported back from APs/user devices. Each AP with its own bandwidth generates a neighbor AP list by overhearing, and reports the information to the APC. Then the APC can generate an invading map among the APs with the neighboring AP lists and bandwidth information. For example,

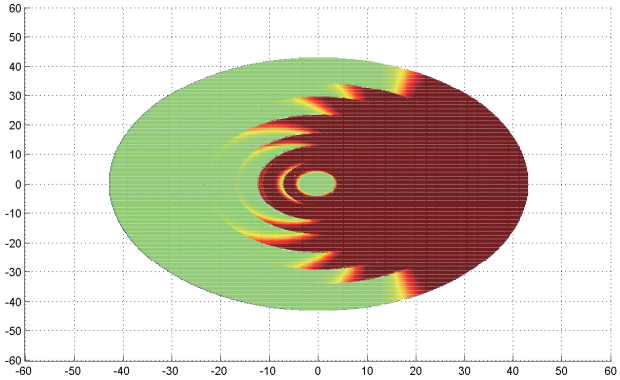

(a) 25m apart

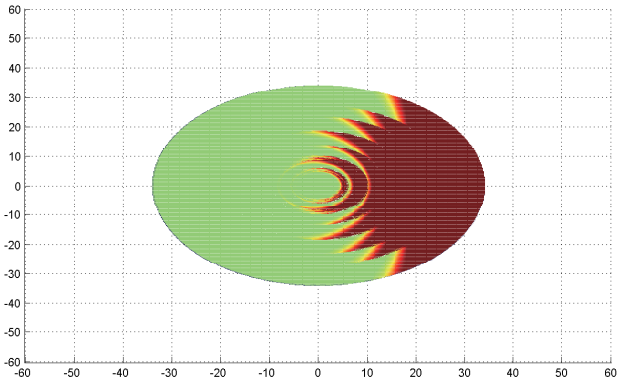

(b) 40m apart

Figure 3.3: PERs of the total and partial invadings between 40MHz and 80MHz senders. x and y axes represent two dimensional coordinates in meters.

if AP a with 80MHz senses the existence of AP b with 20MHz but not vice versa, then the APC can infer that they may suffer partial invading.[3] Note again that we only consider the downlink scenario in this dissertation.

Coloring has been used to solve various network problems in graph theory. In [26, 27, 28, 29], a vertex coloring algorithm is applied for channel allocation that aims to reduce inter-channel interference in an 802.11 legacy network, where partially overlapped channel allocation is allowed. Since 802.11ac does not allow channel overlapping, its channel assignment structure should be different from conventional ones.

Recently, graph modeling is used in CSMA protocol for achieving optimal throughput properties as in [30, 31]. They maintain exclusive usage (coloring) of network resource with the CSMA operation under a single symmetric channel.

We use a special form of graph coloring which is called 'University Course Timetabling (UCT)' [35, 36, 37]. The general UCT problem considers assigning professors to courses and courses to time slots and classrooms while minimizing conflicts, e.g., the number of students who take multiple courses scheduled for a same time period or classroom.

However, the coloring approaches taken so far do not accommodate an asymmetric nature of our problem in multi-channel systems.

[3]Recall that one with smaller bandwidth invades some other one with larger bandwidth in the partial invading.

So we extend the formulation of UCT problem to ours.

The general UCT problem considers assigning professors to courses and courses to time slots and classrooms. A number of versions of this problem with different constraints have been studied [35, 36, 37]. In this subsection, we review a simple version of the UCT problem that aims to schedule courses for time slots in a department of a university.

The number of time slots is fixed to k. The department should avoid scheduling two courses in a same time slot if there are students registering for both courses. A conflict happens between two courses having students in common who are scheduled for the same time period. Since the number of time slots is constrained, it may not be feasible to avoid all conflicts. The objective of this problem is to assign courses to time slots while minimizing the number of conflicts.

The UCT problem can be modeled as a graph coloring problem. Here, courses are vertices in the graph and an edge between two vertices indicates that there will be a conflict if they are scheduled for a same time slot. The conflict level can be expressed as a weight on each edge. The weight can be simply one if they conflict with each other, or the number of students registering for both courses. Assigning a certain color to a vertex means that a course corresponding to the vertex is scheduled for a time slot represented by that color.

Generally, the vertex coloring is one of the combinatorial optimization problems that are known to be NP-hard, and the UCT problem indeed falls in this category as well, and has been shown to be NP-hard

in [35]. This suggests the development of various heuristic algorithms that sacrifice optimality for computational efficiency [37].

Heuristic algorithms to solve the UCT problem with constraints expressed as the number of students registering for two courses in common provide near optimal performance [35]. Since the constraints and conflicts in the UCT problem do not identically match with those of our channel assignment problem, we develop a proper algorithm that aims to maximize the channel utilization while alleviating the HC problem.

3.2.1 Problem Formulation

For modeling, we denote APs by vertices and the interference or invading relations between them by edges. And we denote the channel that an AP chooses as its primary channel by a color. We assume that each AP has decided its bandwidth a priori in some manner. For example, an 802.11a AP can only exploit 20MHz channel while an 802.11ac AP can choose one from all the options. Our objective in the formulation is to assign a color to each vertex to minimize the interference/invading relations to some extent.

Since we omit the case of using 160MHz channel for simplicity, there are four primary channel choices of 20MHz channel and three bandwidth choices as shown in Fig. 3.4. In Fig. 3.4(a), the bandwidths of 1, 2 and 4 represent 20MHz, 40MHz, and 80MHz channels, respectively, and each number in bracket represents the primary chan-

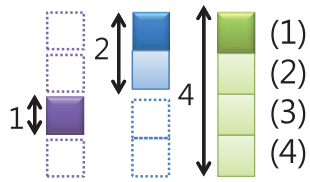

(a) Channel index

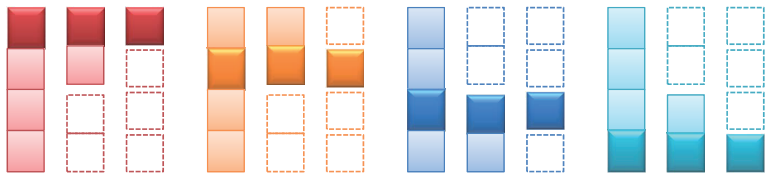

(b) Possible channel configurations

Figure 3.4: Channel index and configurations in the problem formulation.

nel index among four channels. Fig. 3.4(b) shows all possible combinations of the bandwidth and primary channel choices. Here, each filled square represents a chosen primary channel, shaded square a secondary channel, and empty square an unused channel.

An important feature of our channel allocation algorithm lies in how the interactions between these chosen primary channels are dealt with. If both of the APs are with 20MHz channel and their primary channels are not the same, then they are not mutually interfering (i.e. invading) at all. However, if one is with 40MHz channel and the other with 20MHz channel while the secondary channel of the former one is the primary channel of the latter one, they possibly suffer the total invading depending on the distance between them.

To understand the relation between the channels allocated for

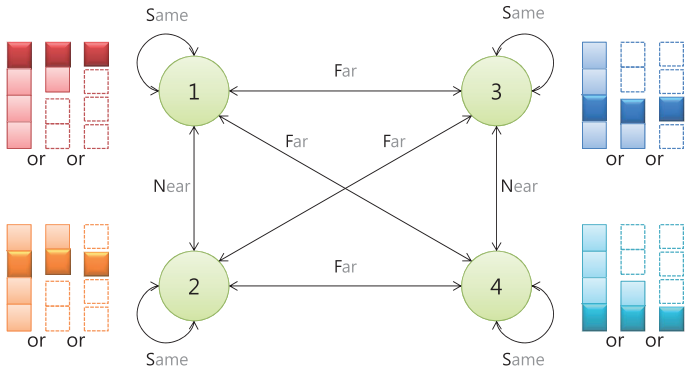

Figure 3.5: Relations between primary channels allocated for neighboring APs. Each number inside a node and on an edge indicates the primary channel index and the channel relation between the primary channels of the two neighboring APs, respectively.

two neighboring APs, we define the (primary) channel relations. In Fig. 3.5, if the two channels have the same (primary) channel index, then the relation is **S** (Same). For the same upper/lower half allocations but not the same channel, it is **N** (Near), and for the different half allocations, it is **F** (Far).

The definition uses non-overlapping-channel and non-separable assumptions in 802.11ac. The channel relations defined in Fig. 3.5 will be used for indicating the cost that will occur when the corresponding channel relation between neighboring vertices is realized. The meaning will be clear if we define a weight vector for each edge as follows.

A weight vector for an edge between two neighboring APs consists of three elements, each of which represents the cost incurred when the channel relation between the primary channels of two neighboring

vertices is 'S', 'N' and 'F', respectively. In other words, the first element is for the channel relation of **S**ame, the second for **N**ear, and the third for **F**ar.

Table 3.2 summaries the weight vectors for all possible pair relations (column 2) according to the geographical distance and bandwidth combinations. The values C_T, C_P, C_M, C_B and C_I are the costs corresponding to the events realized according to the allocated channel relation. C_T is for **T**otal invading, C_P for **P**artial invading, C_M for **M**utually reserving, C_B for mutually **B**lind, and C_I for mutually **I**ndifferent.

When the two APs are close enough, both can reserve/sense the same channel of interest, so they are *mutually reserving*. And if they suffer HC problem, it is a case of either *total or partial invading*. If they interfere with each other but their reserving/sensing ranges do not effectively cover each other, it is a case of *mutually blind*. Lastly, it is denoted as *mutually indifferent* when they are far from each other so that they do not interfere at all.

We represent the costs for C_I, C_M (or C_B), and C_T (or C_P) as '0', '1', and ∞, respectively. If two APs are indifferently positioned, they are not contending, so the cost is 0. And the cost is 1 if they are in mutually reserving or mutually blind relation because they fairly contend for the channel. However, if they suffer HC problem, one of them experiences heavy interference. So we set the cost to ∞ for these cases.

Table 3.2: Weight vectors. (Pair types are in MHz, C_M:Mutually reserving, C_T:Total invading, C_P:partial invading, C_B: mutually Blind, C_I: mutually Indifferent)

Pair type	Pair relation	Weight vector	Example
20&20	mutually reserving	(C_M, C_I, C_I)	$(1, 0, 0)$
	mutually separated	(C_I, C_I, C_I)	$(0, 0, 0)$
40&40	mutually reserving	(C_M, C_M, C_I)	$(1, 1, 0)$
	mutually separated	(C_I, C_I, C_I)	$(0, 0, 0)$
80&80	mutually reserving	(C_M, C_M, C_M)	$(1, 1, 1)$
	mutually separated	(C_I, C_I, C_I)	$(0, 0, 0)$
20&40	mutually reserving	(C_M, C_M, C_I)	$(1, 1, 0)$
	total invading	(C_M, C_T, C_I)	$(1, \infty, 0)$
	partial invading	(C_P, C_B, C_I)	$(\infty, 1, 0)$
	mutually separated	(C_I, C_I, C_I)	$(0, 0, 0)$
20&80	mutually reserving	(C_M, C_M, C_M)	$(1, 1, 1)$
	total invading	(C_M, C_T, C_T)	$(1, \infty, \infty)$
	partial invading	(C_P, C_B, C_B)	$(\infty, 1, 1)$
	mutually separated	(C_I, C_I, C_I)	$(0, 0, 0)$
40&80	mutually reserving	(C_M, C_M, C_M)	$(1, 1, 1)$
	total invading	(C_M, C_M, C_T)	$(1, 1, \infty)$
	partial invading	(C_P, C_P, C_B)	$(\infty, \infty, 1)$
	mutually separated	(C_I, C_I, C_I)	$(0, 0, 0)$

For example, when two APs exploit 20MHz and 40MHz channels (see the pair type of 20&40 in Table 3.2), respectively, and their primary channels are 1 and 2, the channel relation is 'N'. So the second element of the cost vector will have the following (indicated in bold in the table): C_M if they are close enough ('mutually reserving'), C_T if within the invading distance to each other ('total invading'), and C_B if appropriately distant ('mutually blind'), and C_I ('mutually indifferent') if far from each other.

Based on the assumptions and mathematical expressions above, we formulate the problem as an integer programming problem below.

Notations used in the formulation is summarized in Table 3.3.

$$\begin{aligned} \underset{x}{\text{minimize}} \quad & \sum_{i,j} w_{ij}(x_i, x_j; \mathbf{T}, \mathbf{R}, \mathbf{C}) \\ \text{s.t.} \quad & x_i \in \{1, 2, 3, 4\}, \qquad \forall i. \end{aligned} \tag{3.2}$$

We call this problem **PCA** (Primary Channel Allocation) problem and note that the instance of PCA can be represented as $<$ **T,R,C** $>$.

We now prove that the PCA problem is NP-hard. A reference NP-complete problem is "k-colorability".

Definition. k-colorability: For a given graph $G(V, E)$ where V, E are vertex and edge sets respectively, and an integer k, there exists a map $\pi : V \to \{1, 2, ..., k\}$ such that for $(u, v) \in E, \pi(u) \neq \pi(v)$.

The k-colorability is known as an NP-complete problem for any k [25]. Note that the instance of k-colorability can be represented as $< G(V, E), k >$.

Proposition. *The **PCA** problem is an NP-hard problem.*

Proof. Consider an arbitrary instance of 4-colorability problem represented by $< G(V, E), 4 >$. We denote the color assigned to the vertex i of $G(V, E)$ as $x_i \in \{1, 2, 3, 4\}$. For any vertices i and j with $(i, j) \in E$, pair type $t_{i,j}$ is set to '20&20' pair relation $R_{i,j}$ is configured as 'mutually reserving' and the costs are set to $C_I = 0$ and $C_M = C_B = C_T = C_P = \infty$, respectively. Clearly, this reduction from k-colorability $< G(V, E), 4 >$ to PCA $<$ **T,R,C** $>$ requires only the time proportional to the problem size.

Table 3.3: Notations used in the integer problem.

Notation	Description	Condition
$T_{i,j}$	Pair type between AP i and i	$T_{i,j} \in \{20\&20, 40\&40, 80\&80, 20\&40, 20\&80, 40\&80\}$
$R_{i,j}$	Pair relation between AP i and i	$R_{i,j} \in \{$total, partial invading, mutually reserving, separated$\}$
C_T	Cost of Total invading	$0 \leq C_I \leq C_M \leq C_B \leq C_T \leq C_P$
C_P	Cost of Partial invading	
C_B	Cost of mutually Blind	
C_M	Cost of mutually Separated	
C_I	Cost of mutually Indifferent	
x_i	Primary channel of AP i	$x_i \in \{1, 2, 3, 4\}$
$\mathbf{T}$	Pair type matrix	$\mathbf{T} := (T_{i,j})$
$\mathbf{R}$	Pair relation matrix	$\mathbf{R} := (R_{i,j})$
$\mathbf{C}$	Cost matrix	$\mathbf{C} := (C_T, C_P, C_B, C_S, C_I)$
w_{ij}	Weight between AP i and j,	defined in Table 3.2

We need to note that from Table 3.2, $w_{ij}(x_i, x_j; \mathbf{T,R,C}) = 0$ when $x_i = x_j$ and ∞ when $x_i \neq x_j$ for any $(i, j) \in E$ with this setting of **T, R** and **C**. Therefore, an instance of 4-colorability problem can be reduced to an instance of PCA problem in a polynomial time.

If the minimum of PCA $<$ **T,R,C** $>$ is 0, the answer for the 4-colorability problem $< G(V, E), k >$ is 'yes since $w_{ij}(x_i, x_j; \mathbf{T,R,C}) = 0$ for all $(i, j) \in E$, which means that all the adjacent vertices are colored by different colors. On the other hand, if the minimum of PCA $<$ **T,R,C** $>$ is ∞, the answer for the 4-colorability problem $< G(V, E), k >$ is 'no since $w_{ij}(x_i, x_j; \mathbf{T,R,C}) = \infty$ for at least one $(i, j) \in E$, which indicates that some adjacent vertices should be colored by the same color.

This means that if we solve the instance of PCA problem, we can answer the instance of 4-colorability problem as well. Therefore, the considered problem is NP-hard. □

The objective of the PCA problem is to minimize the total cost incurred in allocating a primary channel to each AP while maximizing the channel utilization. As the concept of channel utilization is connoted in the weight vector, minimizing the total cost means that the channel relation between each pair of APs should minimize the number of contending relations and avoid invading relations as much as possible. As it is proven to be NP-hard, we need a heuristic algorithm.

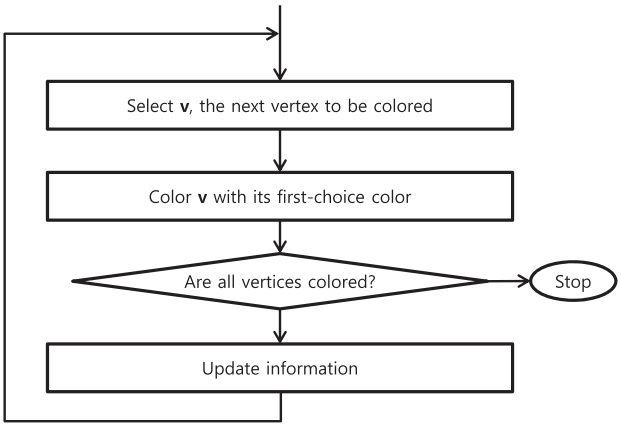

Figure 3.6: A heuristic approach for the vertex coloring.

3.2.2 A Heuristic Primary Channel Assignment Algorithm

In this subsection, we present a heuristic algorithm for primary channel assignment. A basic heuristic approach for the vertex coloring is shown in Fig. 3.6

We define two types of vector metrics for doing this. One is the cost vector for each vertex. The cost vector helps us select which color should be assigned to each vertex.[4] The other is the degree vector for each vertex, which is used to decide which vertex to be colored next, i.e., sequence of vertex coloring. Depending on how these two metrics and edge weight vectors are combined, many heuristic algorithms can be considered. In this work, we consider a simple example to illustrate the procedures of channel allocation.

[4]Our concept is similar to that in [35] but with different definitions.

For the degree vector, we use a vector of two elements for each vertex. The first element of the degree vector is the number of '∞'s in the weight vectors on all the edges that a vertex is connected with. And the second element is the number of '1's on the same edges. The rationale for using these two elements is that with the increase in the numbers of ∞'s (invading relation) and '1's (fair contention), the vertex coloring is becoming more difficult. To avoid invading relations, we put a more weight on the first element than on the second element (reducing the number of contenders). If a tie in the first element occurs, we color a vertex with a larger second element then.

For the cost vector, we use four elements as there are four primary channel choices of 20Mhz each. The first element represents the cost incurred when the first channel is chosen as the primary one, and the second element represents the cost when the second channel is chosen, and so forth. A vertex with the lowest cost element is colored since our objective is to minimize the total cost. When multiple colors are with a same lowest cost, choose one randomly.

For example, consider two neighboring vertices A and B with the edge weight vector, (w_s, w_n, w_f) and assume $w_s > w_n > w_f$. Initially, vertices A and B both have the cost vector (0,0,0,0). Assume node A is assigned first color 2. Then vertex B will have the primary channel relation with A as 'N', 'S', 'F', and 'F' according to the allocated channels of 1, 2, 3, and 4, respectively, as four channels are available. From the edge weight vector of (w_s, w_n, w_f), vertex B will have the

cost vector of (w_n, w_s, w_f, w_f). Refer to Fig. 3.7 too.

Then the algorithm selects a next vertex by comparing the degree vector of each vertex to be allocated, and assigns it a color that shows a minimum value among the four elements in its cost vector. The procedures stop when all the vertices are colored. In the previous example, the minimum element value among w_n, w_s, w_f and w_f for vertex B is w_f. So vertex B will be assigned channel 3 or 4, randomly.

In Fig. 3.7, we consider an example of channel allocation for a topology of 6 APs, where we denote an AP exploiting 80MHz channel by a largest circle, 40MHz one by a medium sized circle, and 20MHz one by a smallest circle, respectively. And simply connected edges and directed edges represent mutually reserving relation and invading relation, respectively. For comparison, we use the RSSI based primary channel selection algorithm, in which each AP selects a channel with a lowest RSSI as its primary one. The RSSI-based scheme emulates a channel selection method in the legacy versions of 802.11 which chooses the best channel as its operating one. For simplicity of illustration, the number of active neighbors on each channel is used as a channel selection metric for the RSSI-based algorithm.

Figs. 3.7(b) and 3.7(c) illustrate the allocation results of the heuristic algorithm and the RSSI based algorithm, respectively. Also, for the comparative study, we show the optimal allocation results in Fig. 3.7(d) which are obtained by brutal force calculation for a small size network.

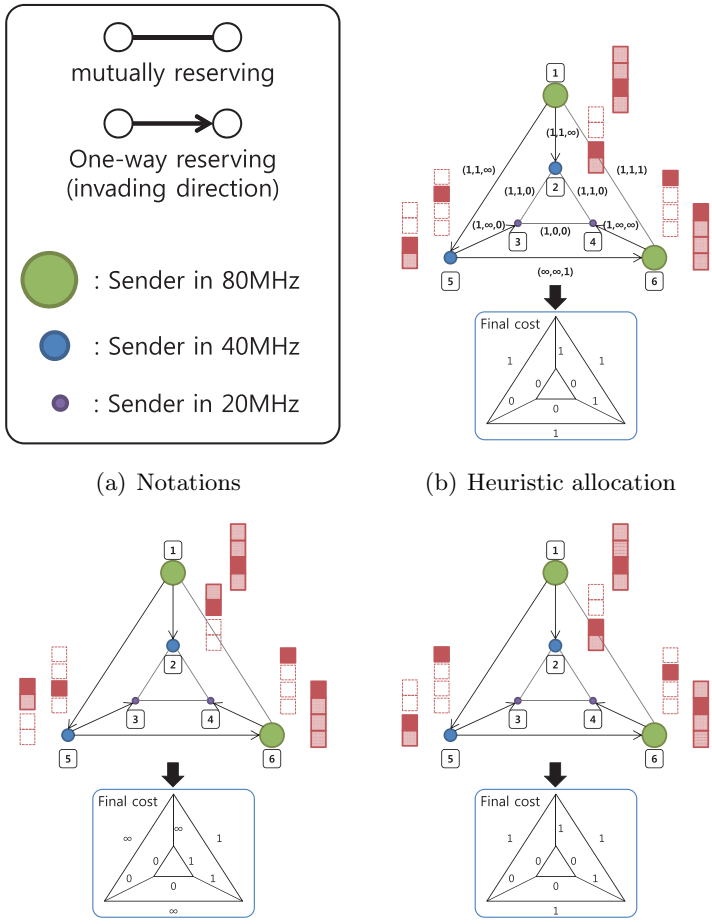

(a) Notations

(b) Heuristic allocation

(c) RSSI based allocation

(d) Optimal allocation

Figure 3.7: An example of channel allocation for comparison.

Table 3.4: Channel allocation example of the heuristic algorithm. ($I = \infty$)

Vertex	6	5	1	4	2	3
Degree	[4 5]	[4 4]	[2 7]	[2 4]	[1 6]	[1 4]
1^{st}	⓪**000**	0000	0000	0000	0000	0000
2^{nd}		***II***①**1**	1111	1III	0000	0000
3^{rd}			***II***②**2**	1III	0000	001I
4^{th}				①***III***	II11	001I
5^{th}					***II***①**1**	101I
6^{th}						**1**⓪**2*I***
Result	Ch.1	Ch.3	Ch.3	Ch.1	Ch.3	Ch.2

For our algorithm, we give the procedures in Table 3.4. Since vertex 6 has a largest first element in the degree vector (i.e. 4 but a tie with vertex 5) and a larger second element (i.e. 5) compared to vertex 5, it becomes the first one to be colored. And vertex 3 has the lowest value (i.e. 1 but a tie with vertex 2), and it has a smaller second element (i.e. 4) compared to vertex 2. So it becomes the last one to be colored.

Vertex 6 is randomly assigned color 1 first, which is channel 1, because the cost vector is filled with all zero elements (i.e. equal). In the third row and second column, the circled first element (i.e. 0) indicates the chosen channel number '1' for vertex 6. Then the cost vectors of vertices 1, 4 and 5 are updated since they are the neighbors of vertex 6.

The weight vector on the edge between vertices 6 and 5 is $(\infty, \infty, 1)$, each of which represents the cost to be incurred if a channel relation of 'S','N' or 'F' with vertex 6 is assigned to vertex 5. So, the updated cost

Table 3.5: Channel allocation example of the RSSI based algorithm.

Vertex	6	5	1	4	2	3
1^{st}	⓪**000**	0000	0000	0000	0000	0000
2^{nd}		①**111**	1111	1111	0000	0000
3^{rd}			**22**①**1**	1111	0000	1100
4^{th}				①**111**	1111	1101
5^{th}					**2**①**11**	2101
6^{th}						**32**⓪**1**
Result	Ch.1	Ch.1	Ch.3	Ch.1	Ch.2	Ch.3

vector for vertex 5 becomes $(\infty, \infty, 1, 1)$. In the same manner, the updated cost vectors for vertices 1 and 4 are $(1, 1, 1, 1)$ and $(1, \infty, \infty, \infty)$, respectively.

The updated cost vectors are shown in the fourth row. Then vertex 5 is colored in the third row. As vertex 5 has the lowest cost value for the third element, it is assigned channel 3. Then the cost vectors for vertices 1 and 3 are updated in the same manner, and shown in the fifth row. Since there are six vertices, the coloring and updating cycles are performed six times. After coloring vertex 3, the algorithm stops. The allocation results are given in the bottom row, and also shown in Fig. 3.7(b) with filled rectangles.

Table 3.5 shows an example of the RSSI based allocation algorithm operation with the same vertex coloring order as in our proposal. Each element in the cost vector represents the number of active neighboring APs in the corresponding channel. Each vertex chooses a channel with a lowest number of active APs as its primary one.

The final costs for the comparative schemes are shown in Fig. 3.7.

The proposed heuristic method and the optimal method show the same cost while the RSSI-based one permits invading relation at three edges. The heuristic allocation and the RSSI based allocation have the same computational complexity of $O(n^2)$ while the optimal allocation is NP-hard. This suggests that our heuristic algorithm works well at least for reasonable size networks.

3.3 Simulation Results

In this section, we present the simulation results in terms of error rate, throughput and fairness.[5] We compare the heuristic algorithm with random, RSSI-based, and exhaustive (optimal) allocation. The random allocation selects a primary channel for each AP randomly (i.e., in an uncoordinated manner). The RSSI-based one allocates a channel with the lowest RSSI for each node and emulates a channel selection method in the legacy versions of 802.11. The optimal allocation uses the result of the exhaustive search of Eq. 3.2. Since the integer programming is NP-hard, the optimal allocation is infeasible in polynomial time. For this reason, we obtain the allocation results for up to 10 APs.

Throughout the entire simulations, the slot time, DIFS, PIFS, and SIFS are set to $9, 34, 25$, and $16\mu s$, respectively, and the transmission

[5]None of the available simulators (NS2, NS3, etc.) so far implements the 802.11ac contention mechanism in multi-channel environments. So, we implemented it with C++ in the same way that NS2/3 implements the simulator (Event-queue based 'event driven simulator').

power is fixed to 17dBm. We assume that the inter-transmission-attempt-time is $100\mu s$ and the packet length is 1500bytes. The transmission time depends on the selected MCS (Modulation and Coding) level and number of control messages (RTS, CTS and ACK) with PLCP (Physical Layer Convergence Protocol) overhead of $20\mu s$. Packet error events are emulated with PER values calculated from SINRs as in Section 3.1.

3.3.1 Case for a Network with Two APs

Fig. 3.8 presents the throughput performance of the heuristic algorithm in a simple invading scenario. In the considered scenario, two transmitting APs of 40MHz (invader) and 20MHz (victim) are located a certain distance apart and each AP's receiver is positioned randomly between those two APs. Each simulation is performed 100 times and the simulation time is 1s. Then the empirical CDF (Cumulative Distribution Function) of throughput is measured.[6]

In Fig. 3.8(a), we show the throughput improvement of the heuristic algorithm compared to the random and RSSI-based allocation algorithms when the victim and the invader are 30m apart. The RSSI-based allocation shows better performance than the random one because it helps 20MHz PPDU and 40MHz PPDU avoid each other orthogonally in the 80MHz band. The CDF shows a stair-like shape because the AMC scheme discretizes the throughput space. The

[6]The results for other combinations of bandwidth choice show a similar tendency, and are omitted due to the page limit.

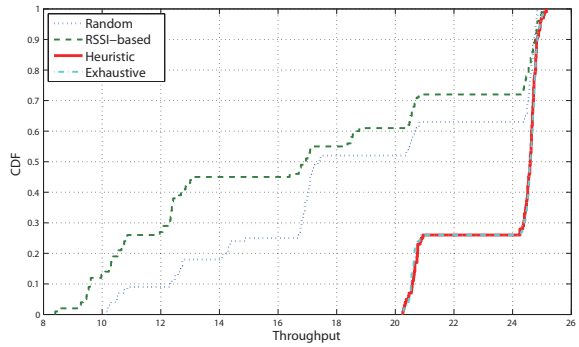

(a) 30m apart

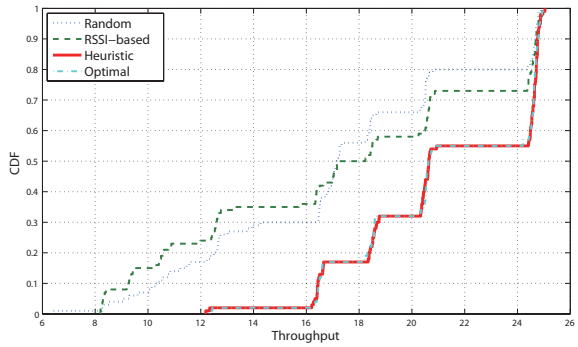

(b) 40m apart

Figure 3.8: Empirical CDF of the victim's throughput according to the distance between the invader and the victim.

(a) A 6-chain topology

(b) Random allocation result (231434)

(c) RSSI-based allocation result (313121)

(d) Heuristic allocation result (113113)

(e) Exhaustive allocation result (311311)

Figure 3.9: A chain topology and bandwidth allocation results.

heuristic algorithm shows the identical result with the exhaustive.

Fig. 3.8(b) shows the same results except that the performance improvement is reduced and the RSSI-based allocation shows a bit better performance than the random allocation to some extent. The reasons are that their invading intensity decreases with their separated distance and the AMC scheme runs properly, respectively.

3.3.2 Case for a Chain Topology with Six APs

Fig. 3.9 shows a simple chain topology of 6 transmitter-receiver pairs indexed by 1 through 6. The transmitters are on a straight line and the receivers are positioned on another straight line which is 20m below

Table 3.6: Tx. trial, error rate and throughput of each node in the 6-chain topology. Tx. (#), Err. (%) and Thr. (Mbps).

Tx. (#)		1	2	3	4	5	6	Overall
Random	Tx.	2359	1787	1655	1619	1597	1536	10553
	Err.	0.00	64.91	0.06	0.00	0.31	55.14	19.08
	Thr.	28.31	7.52	19.85	19.43	19.10	8.27	102.05
RSSI-based	Tx.	2370	1783	1652	1582	1614	1542	10543
	Err.	0.00	67.13	0.18	0.00	0.12	56.74	19.70
	Thr.	28.44	7.03	19.79	18.98	19.34	8.00	101.58
Heuristic	Tx.	1626	1591	1653	1604	1599	1810	9883
	Err.	0.00	0.25	0.43	0.00	0.13	0.00	0.10
	Thr.	19.51	19.04	19.75	19.25	19.16	21.72	118.44
Exhaustive	Tx.	1594	1605	1659	1586	1637	1804	9885
	Err.	0.00	0.12	0.30	0.00	0.00	0.00	0.07
	Thr.	19.13	19.24	19.85	19.03	19.64	21.65	118.54

the transmitters. Their relative distances are configured to suffer HC problem so that node 1 invades node 2, node 2 invades node3 and so on. Because of their bandwidth usages (80, 40, 20, 80, 40 and 20), each pair of nodes suffer 'Total', 'Total', 'Partial', 'Total' and 'Total' invadings, respectively. Also, the results of the competitive bandwidth allocation algorithms are shown in the figure. The random and RSSI-based algorithms happen to be not able to avoid the invadings from 1 to 2 and 5 to 6 while the heuristic and exhaustive ones do.

The simulation results for the chain topology are summarized in Table 3.6 in terms of number of transmission trials, error rate and throughput. As shown in the table, high packet error happens at node 2 and node 6, so their throughputs decrease. In the random and RSSI-based allocation schemes, the number of transmission trials for node 1 is much higher than those for the other nodes. This is because node 1 does not sense any other nodes nearby, thus attempts to transmit all the time. The rest of the nodes have at least one contender, so they

possibly defer their transmissions. A proper channel allocation leads node 1 to sense node 2, so the trial number for node 1 becomes similar to those for the others in the heuristic and exhaustive schemes. Node 6 shows relatively higher throughput for the heuristic and exhaustive schemes because they have no contender.

We can see that the throughput increases about 15% and the error rate drops 19 percentage point in the chain topology. The error rate reduction in the considered topology is rather great. However, the performance improvement depends heavily on the network topology, so we perform simulations for random networks in the following.

3.3.3 Case for Various Sized Random Networks

We consider N APs and N user terminals randomly located in a 100m $\times$ 100m grid topology. Each AP, with randomly chosen bandwidth, is associated with a randomly distributed user terminal nearby. The following results are the averages of 100 repeated simulations and each simulation time is 1 second.

Fig. 3.10 presents the performance comparison in terms of network-wide PER, throughput, and fairness. The heuristic algorithm lowers PER by 7 percentage point at maximum compared to the random and RSSI-based allocation schemes as shown in Fig. 3.10(a). The random and RSSI-based allocation schemes show almost the same performance because each AP chooses a primary channel in a greedy manner without considering others' choices. And our heuristic al-

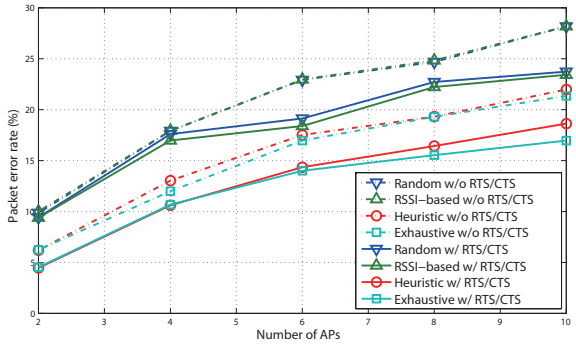

(a) Packet error rate

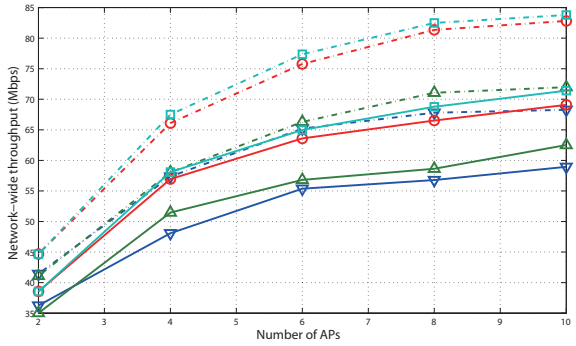

(b) Network-wide throughput

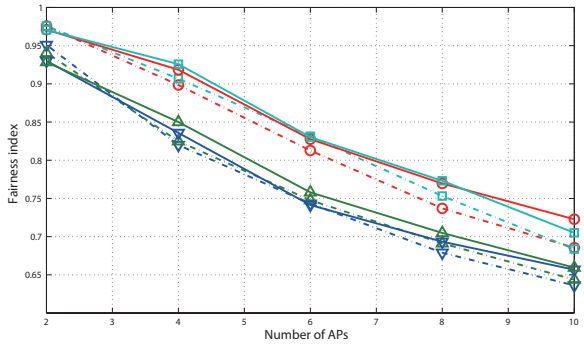

(c) Jain's fairness index

Figure 3.10: Network-wide packet error rate, throughput and fairness performance in small sized networks.

gorithm shows near optimal performance. The enhanced RTS/CTS handshake avoids collision by reserving spaces at both the transmitter and receiver sides, which also results in around 4 percentage point improvement. However, it also suffers from the HC problem since RTS/CTS messages are also transmitted with a fixed transmission power regardless of the bandwidth usage. Therefore, our channel allocation approach along with the enhanced RTS/CTS scheme shows the best performance.

The lower PER leads to the improvement of throughput performance as shown in Fig. 3.10(b). The network-wide throughput improves at most 17%. The collision avoidance effect of the RTS/CTS scheme does not lead to throughput improvement, since it causes the exposed terminal problem which leads to reduced transmission attempts. So our channel allocation approach without the RTS/CTS scheme shows the best performance. This leads us to conclude that the RTS/CTS scheme lowers PER at the expense of throughput. Fig. 3.10(c) shows throughput fairness performance. The RTS/CTS scheme does not have a significant impact on the performance while the channel allocation approach has.

Fig. 3.11 shows the same performance evaluation results for a 200m $\times$ 200m topology with more APs. Since the exhaustive search is not feasible for a large number of APs, it has been excluded from the evaluation. In the figure, PER and throughput performances show similar results.

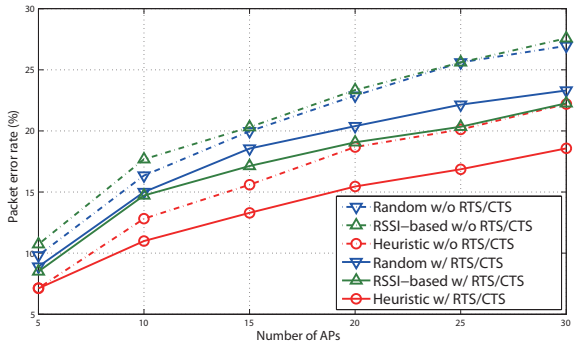

(a) Packet error rate

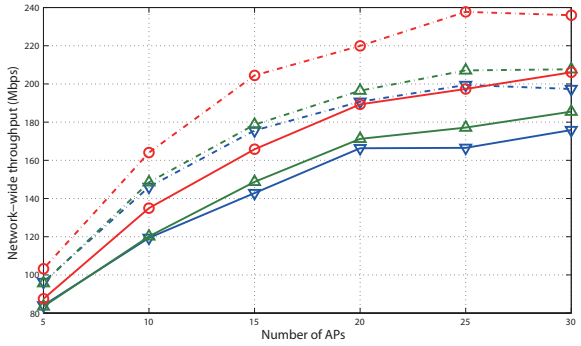

(b) Network-wide throughput

Figure 3.11: Network-wide packet error rate, throughput and fairness performance in large sized networks.

Note that the results so far are obtained from the averages of all the nodes in the network. While 7 percentage point improvement of PER does not influence a single user experience significantly, there are some nodes whose transmissions are highly interfered, and thus corrupted by others' in the invading scenario. We directly show the performance improvement on those victims in Fig. 3.12.

Fig. 3.12(a), the CDF for PERs of all transmission pairs is shown. As it can be seen, our heuristic algorithm significantly lowers the distribution of PER and shows near optimal performance. As before, the random and RSSI-based schemes show similar performances.

The throughput increment ratio of our proposal for a particular AP which gets the minimum throughput among all APs is shown in Fig. 3.12(b). The performance of the worst throughput user greatly improves under all cases. While the results fluctuate heavily, the general tendency that the ratio increases with the number of APs can be observed. This is because as the network gets congested, the worst-performing AP has more influencing invaders, and alleviating this situation improves the throughput performance more. These minimum throughput and packet error rate results prove that the heuristic allocation algorithm lessens the invading problem, thus leading to improved fairness performance, as in Fig. 3.10(c).

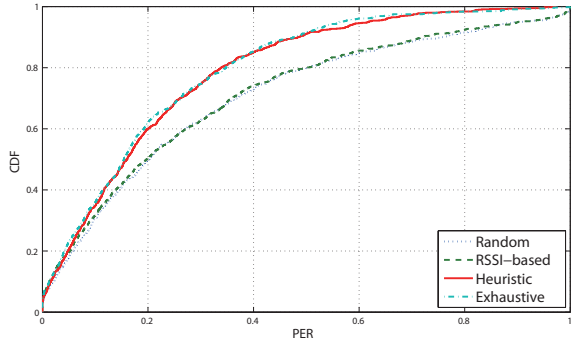

(a) CDF for PER with RTS/CTS when $N = 10$

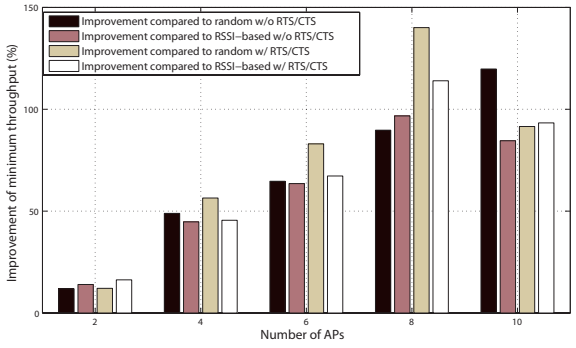

(b) Throughput increment ratio of a node with the worst throughput

Figure 3.12: CDF for PER when $N = 10$ and throughput increment ratio.

3.4 Summary

As a first solution to the hidden channel problem, the *PCA* algorithm is proposed in this chapter. While formulating the channel allocation problem and running the simulations, the PER behaviors when some parts of the bandwidth are interfered by other transmission studied in the beginning of this chapter are used to make the problem and simulation more realistic. The channel allocation problem is formulated using graph theory and proven to be NP-hard. Then the PCA algorithm, which is heuristic, is proposed. Using simulation, we show that the PCA lowers the packet error probability which leads to the enhanced throughput performance of a network. Also, fairness of the network can be boosted.

The channel allocation problem formulated in this chapter assumes that the bandwidth of each link or AP is fixed by some reasons. In the following chapter, we break this assumption. And we propose another solution to the hidden channel problem by modifying the bandwidth dynamically.

Chapter 4

PoBA (Post-CCA based Bandwidth Adaptation)

4.1 Introduction

In this chapter, the effect of the bandwidth selection is firstly presented in general. Then the post-CCA operation, another clear channel assessing procedure after finishing a transmission is proposed followed by the *PoBA*, post-CCA based Bandwidth Adaptation algorithm. Then the performance enhancement of the PoBA is shown using simulation.

Fig. 4.1 shows MCS (Modulation and Coding Scheme) levels and corresponding receiver sensitivities defined in 802.11ac. Receiver sensitivity is the minimum received signal power required for decoding a signal with error probability of smaller than 10%. So, the required re-

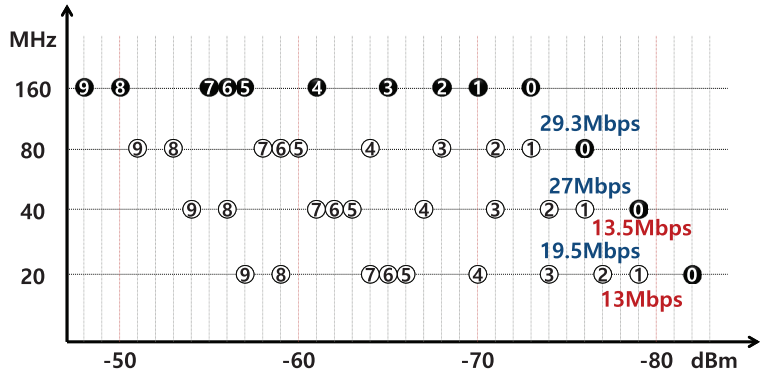

Figure 4.1: Ideal MCS levels on each bandwidth according to receiver sensitivity, where the number in a circle represents the MCS level and the x-axis is the required receiver sensitivity.

ceiver sensitivity can be considered as an ideal channel condition (i.e., only with path loss attenuation). Intuitively, a higher MCS level requires a higher receiver sensitivity for correct decoding.

As the figure shows, using a wider bandwidth with the same MCS level requires better channel condition. In other words, for a given channel condition, we need a lower MCS level if we want to use a larger bandwidth. On the other hand, from the perspective of achievable throughput, it is always best to use the largest bandwidth possible. For example, when the channel condition is -82dBm, there is only one option of MCS level 0 at 20MHz bandwidth. As for -79dBm, the viable options are MCS 1 at 20MHz and MCS 0 at 40MHz. The theoretical data rates at each option are 13Mbps and 13.5Mbps, respectively. Likewise, if the channel condition is -76dBm, there are three options, MCS 2 at 20MHz, MCS 1 at 40MHz, and MCS 0 at 80MHz, with

data rates 19.5, 27 and 29.3Mbps, respectively. Therefore, using a wider bandwidth is always better and the best options are indicated by black circles in Fig. 4.1 .

However, using a larger bandwidth comes at some disadvantages. First, it results in the reduced transmission range. Since the transmission power is fixed due to the restriction at the power amp, using a wider bandwidth reduces the power spectral density of each transmission. For instance, if 100mW is used for transmission, then 5mW per MHz and 2.5mw per MHz are the power spectral densities of 20MHz and 40MHz bandwidth, respectively. Since the channel attenuation and fading are multiplied and noises are added on the entire bandwidth that a transmission occupies, using a larger bandwidth lowers SNR (Signal to Noise Ratio), i.e., the decreased transmission range or degraded packet reception probability. In other words, using wider bandwidth yields lower power spectral density.

This disadvantage leads to the second one. The range of a transmission on a wider bandwidth becomes shorter, thus reducing the spatial area that the transmission reserves through CSMA/CA. So, if there is another device outside the reserving range of a transmitter, then the packet in transmission suffers from potential interference. This problem did not happen until 802.11ac was introduced, because all the devices used the same bandwidth and power. However, in 802.11ac with non-overlapping channelization, the heterogeneous bandwidth usage leads to the imbalance between the reservation

capabilities [12, 15].

4.2 Experimental Results

We have conducted simple experiments to demonstrate that the hidden channel problem is real. We measure the differences in power spectral density in accordance with different bandwidth usages, and in the results of channel assessment as a function of physical locations of a transmitter, a receiver and an interferer. All these affect the results of contention and transmission.

$$RSSI(dBm) = (200/3069) \cdot RSSI_D - c$$
$$c = \begin{cases} 280/3 & \text{gain = high} \\ 155/2 & \text{gain = medium} \\ 126/2 & \text{gain = low} \end{cases} \tag{4.1}$$

USRP N200 with GnuRadio [1, 3] and WARP v.3 with WARPLab reference design version 7.5.1 [2] are used in our experiments. The WARP v.3 uses MAX2829 transceiver hardware [4]. The ADC and DAC in the MAX2829 have an intrinsic curve for converting RSSI (Received Signal Strength Indicator) values from the hardware to the digital value, as the above equation, depending on antenna gain. Here, $RSSI$ is in dBm and $RSSI_D$ is the digitized RSSI value that the ADC returns.

First, we measure the spectral densities for 10MHz and 20MHz transmissions with a fixed power. A WARP board transmits a packet, and its spectral density is measured by a USRP board which is 0.5m away from the transmitter. Since the stably supporting bandwidth of the WARP board is 20MHz at 5GHz band,[1] we use 20MHz for a full band transmission and 10MHz for a half band one in the following experiments without loss of generality. Both the interpolation [14, 15] and the sub-carrier nulling [16] are used to control bandwidth, and they yielded the same results.

Fig. 4.2 plots power spectral density (PSD) while varying the bandwidth, where the unstable lines at the bottom are the PSD at a specific point in time and the stable lines at the top are peak holding graphs that store the maximum PSD over time. As shown in the figure, the PSD with the full bandwidth is around -45dBm while that with a half bandwidth is approximately -40dBm. This result simply verifies that using a narrow bandwidth concentrates the entire power on the narrow bandwidth, which results in higher PSD compared to using a wider bandwidth.

Fig. 4.3 shows the topologies used in the next experiment in which 3 WARP boards are used to create a simple transmitter–receiver (Tx–Rx) pair with an interferer (Ix). Topology 1 is for an equal distance scenario, topology 2 for a close Tx–Rx scenario, topology 3 for a close

[1] A WARP hardware supports up to 40MHz bandwidth. However, when a packet is sent in 40MHz bandwidth at 5GHz with the WARPLab reference design, it suffers from a higher bit error rate.

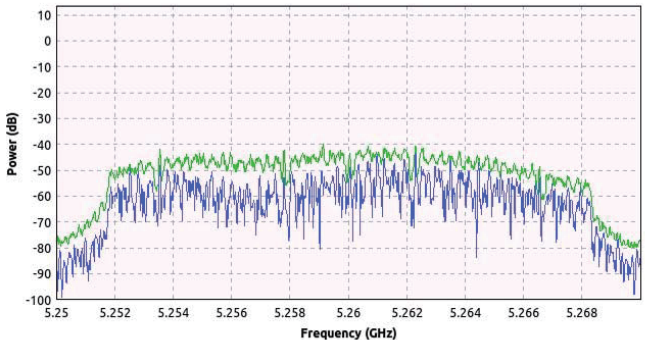

(a) PSD of fullband transmission (20MHz)

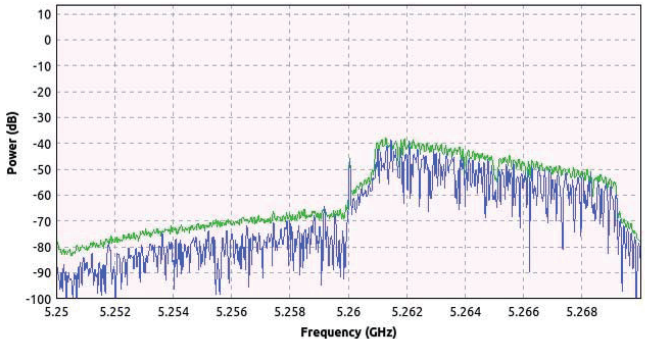

(b) PSD of halfband transmission (10MHz)

Figure 4.2: Power spectral density of full and half band transmissions.

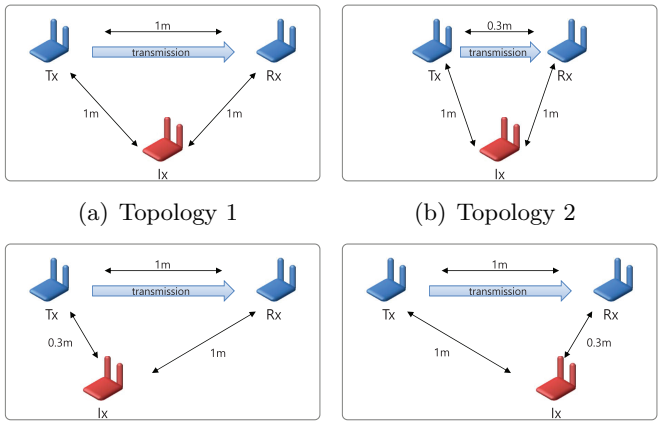

(a) Topology 1 (b) Topology 2

(c) Topology 3 (d) Topology 4

Figure 4.3: Experimental topologies.

Tx–Ix scenario, and topology 4 for a close Rx–Ix scenario. The Tx–Rx pair use full bandwidth and the Ix occupies only a half bandwidth. The Tx and Ix transmit simultaneously to measure the CCA results and bit error rates. The averages with the standard deviation bars are shown in Fig. 4.4, where each point is obtained from 100 repeated measurements.

Fig. 4.4(a) shows the CCA results for different topologies, where the conventional CCA is the one performed right before starting a transmission and the Post-CCA is another channel assessment after completing a transmission. The conventional CCA results are shown at both Tx and Ix and the post-CCA results are shown on both of the half channels.

As shown in Fig. 4.4(a), the post-CCA results on the interfered half channel show much larger values than those on the other inter-

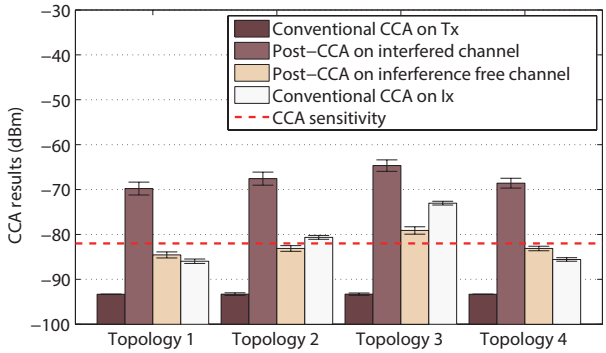

(a) Conventional CCA and Post-CCA results on both of the half channels at Tx and CCA results at Ix while Tx is transmitting

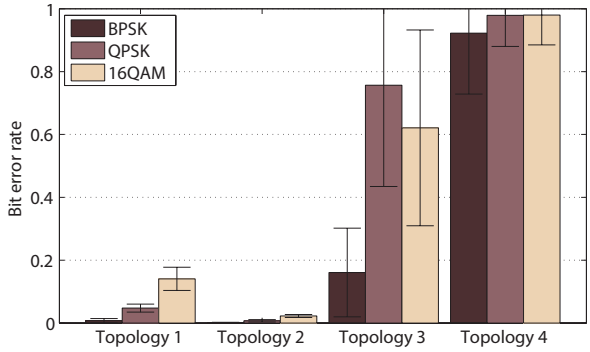

(b) Bit error rates of BPSK, QPSK and 16QAM modulations on each topology when there is hidden channel interference

Figure 4.4: Experimental results for different topologies.

ference free one. This is a simple, expected result since the interference occupies only half of the channel. The post-CCA results on the interference free half-channel should be similar to the conventional CCA results, which is nearly -90dBm in the experiment. However, in Fig. 4.2(b), there exists some power leakage on the interference-free half channel due to the imperfection of bandwidth control software and hardware in our experiment.

Also, note that conventional CCA results at the Ix side during the Tx's transmission are also different from post-CCA results at the Tx side. This gap implies unbalanced CCA capabilities of Tx and Ix. The dotted line in Fig. 4.4(a) represents the primary CCA sensitivity level, -82dBm. Above (below) the sensitivity level is the region for the channel busy (idle). During the Tx's transmission, Ix cannot detect the existence of the transmission on topologies 1 and 4. However, on the same topologies, Tx is aware of the existence of Ix's transmission through the post-CCA results on the interfered half channel. This implies that Ix interferes with Tx all the time on the half channel due to the failure in busy channel detection. That is, the hidden channel problem occurs.

The corresponding bit error probabilities are plotted in Fig. 4.4(b) when Ix interferes with Tx. Since the error rates without interference are nearly zero on all the topologies, the results represent additional bit errors caused by Ix. As shown in the figure, the severity of the problem depends on the modulation level. A higher modulation level,

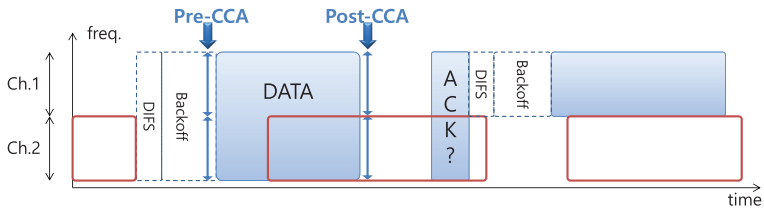

Figure 4.5: Post-CCA operation.

Table 4.1: Post-CCA observations and intuitions.

Observation		Intuition
Post-CCA	ACK?	
Idle	Yes	Working well
Idle	No	Fading error
Busy	Yes	Collision but working well
Busy	No	Hidden channel collision error

which is used when the channel condition is good, is more prone to the interference. These experiments show the discrepancy in the CCA capability of different bandwidths, and also show that the discrepancy and the physical topology affect transmission bit error rate greatly.

4.3 Post-CCA & PoBA

In this section, we propose a solution to the hidden channel problem, called *PoBA* (Post-CCA based Bandwidth Adaptation), which uses post-CCA for bandwidth adaptation.

4.3.1 Post-CCA Operation

The intuition behind the post-CCA operation and the corresponding bandwidth adaptation, PoBA, is that an 'interferee' can sense its 'in-

terferer', but not vice versa, and hence the interferee should avoid collision. Fig. 4.5 illustrates the post-CCA operation in a simple two channel scenario, where the filled solid squares represent interferee's channel occupancy and the empty solid squares represent interferer's.

The interferee starts to back off right after the interferer finishes its transmission. Upon sensing the entire channel idle, the interferee starts transmission. But, the interferer also starts its own since it is unable to sense the channel busy. With the post-CCA operation, the interferee is aware of the existence of a disrupting transmission on channel 2. If no ACK packet is received in time, the interferee concludes that the transmission has failed due to a hidden channel collision.

Table 4.1 shows the interferee's speculations about the network condition according to the observations from post-CCA and whether an ACK is received correctly. Here, we are interested in when the post-CCA tells that some channels are busy and an ACK has not been received in time. The other cases are usual scenarios as in homogeneous bandwidth networks.

If the interferer's transmission ends before the interferee's, the post-CCA cannot detect the interferer's existence. Clearly, the duration of the interferer's transmission affects the performance of the post-CCA operation. If its duration is relatively short, a transmission failure will be considered as a channel fading error. We leave this case to the responsibility of AMC (Adaptive Modulation Coding) and

FEC (Forward Error Correction) scheme which combat bad channel condition.

After finishing a transmission, a transmitter switches its antennas from transmit mode to receive mode to wait for an ACK packet. So, post-CCA operation is not a new operation because the conventional operation just has not made use of the information that has been available. Or, it has not been needed since spectral reservation (not spatial) was assumed to work well in homogeneous bandwidth networks.

High throughput WLAN standards, i.e., 802.11n, 802.11ac and 802.11ax, adopt OFDM/OFDMA as a basic physical-layer scheme. The granularity of resource management/scheduling is a sub-carrier or a sub-channel in OFDM. Via FFT (Fast Fourier Transform), it is possible to measure idleness of each subcarrier if proper CCA sensitivity per subcarrier is defined. So, the idea of post-CCA can be applied to OFDM. Here we use a 20MHz channel as the unit of resource management, and hence we only suggest per-channel post-CCA. Designing a proper clear sub-carrier assessment is a separate open issue for future 802.11 systems.

The post-CCA operation helps a transmitter assess network condition like CSMA/CD in the wired Ethernet. In a wired network, a transmitter can detect other signals during the transmission of a packet. The post-CCA operation cannot enable collision detection during transmission, but helps improve assessment of channel condi-

tion by sensing the channel once more after completing a transmission. Albeit different, they share a similar concept of re-assessing channels after starting a transmission.

CSMA/CD aborts transmission if a collision is detected. However, a different approach should be taken in wireless systems since no other action can be taken during a transmission. Next we present a bandwidth adaptation algorithm, PoBA, to alleviate the hidden channel collision problem.

4.3.2 PoBA Algorithm

Recently, researchers have studied feasibility of dynamically changing bandwidth without modifying hardware, i.e., by only manipulating digital signal processing stages [14, 15, 16]. They claim that agile expansion or reduction of bandwidth according to the medium condition enhances the efficiency of transmissions. We use their methods of controlling bandwidth by adding an additional signal processing step, such as an interpolation or a subcarrier nulling block at the digital baseband processing stage.

Fig. 4.5 also illustrates an example of bandwidth reduction based on the post-CCA. In the figure, the interferee is aware that channel 2 has been interrupted from the middle of the transmission until the end. So, the interferee changes its bandwidth from using both channels to only channel 1 in the following transmission. Then, the interferee and the interferer use only one of the two channels, and hence no more

collision.

Before detailing the algorithm, we address how a transmitter and a receiver agree on the same channel configuration (i.e., primary channel and bandwidth), when the transmitter initiates bandwidth adaptation. One can assume that they share the same channel configuration before bandwidth adaptation is triggered. There are a number of ways for rendezvous of the transmitter and the receiver.

First, the transmitter initiates bandwidth adaptation by sending a preamble sequence. 802.11ac defines a different preamble sequence for each bandwidth [9]. So, by sending a packet with a bandwidth-specific preamble, the transmitter informs its receiver that the bandwidth has been changed. For this purpose, the receiver must be ready to receive any possible bandwidth-specific preambles.

Second, each AP transmits a beacon message periodically that contains a control field to indicate its bandwidth and primary channel number [9]. This control field can be also used for rendezvous in a cell.

Another method is through enhanced RTS/CTS messages as in Fig. 2.3. A transmitter sends RTS messages only on desired channels, then the receiver responds with CTS messages on those channels. In this dissertation, we assume that a transmitter–receiver pair agree on the same channel configuration through one or a combination of the above methods.

We assume the maximum bandwidth to be 80MHz since it is the

mandatory supporting bandwidth. The following PoBA algorithm can be extended to bandwidth of 160MHz without loss of generality. Under this assumption, there are three bandwidth options: 20MHz, 40MHz and 80MHz. Recall that there are two 40MHz channels and four 20MHz channels in a single 80MHz channel as shown in Fig. 2.1. Besides bandwidth variation, channel location is another factor to be considered. Thus, we define four different actions — *reducing, expanding, exploring* and *staying* — for which Fig. 4.6 shows case-study examples.

Reducing bandwidth is to relinquish some part of the bandwidth because of the hidden channel collision on it while bandwidth is expanded/enlarged for one of two cases. The first case is to face the hidden channel intrusion from another transmitter that uses a wider bandwidth as in Fig. 2.5(a). This case happens due to discrepancy between the CCA sensitivities on the primary and secondary channels. If the interferee reserves channels which are secondary for the interferer, the reservation may not be successful because the secondary channel(s) requires more power to assess busyness. In such a case, matching the bandwidth with the interferer's solves the reservation asymmetry by sharing their primary channel. We incorporate the cases with and without discrepancy by controlling the probability of taking an expansion action.

The second case is to maximize channel utilization. As discussed earlier, it is better to use a wider bandwidth possible if there is no

interference. So, when the transmission is successful, our algorithm expands the allocated bandwidth with a predefined perturbation probability, ϵ_{per}^{bw}, to make use of available bandwidth as much as possible. In both cases, the expansion is a viable option, if possible. Recall Fig. 4.1 where increasing bandwidth is not possible when the ideal channel condition is not good. For example, if the ideal channel condition is -82dBm, the only viable option is 20MHz. In such a case, the probability for expanding bandwidth is set to zero.

Exploring is to try some other channels with the same bandwidth. The entire bandwidth can be interrupted by the hidden channel problem on each channel from multiple interferers in dense networks. Also, a possible way of avoiding a partial hidden channel collision is to try different channels at different locations, i.e., exploring other channels. For these purposes, the exploration action allows channels to move to another location with the same bandwidth. Staying is to keep current channel configuration again.

Fig. 4.6 shows case studies for each of the actions mentioned above, where 'staying' options are not shown, filled squares represent locations of primary channels, shaded squares are for secondary channels, empty squares are for unallocated channels, and big arrows represent hidden channel collision from an interferer to an interferee.

Each case illustrates a possible channel configuration of hidden channel collision, and actions show possible channel switching options that the interferee can take. Channel configurations right next to the

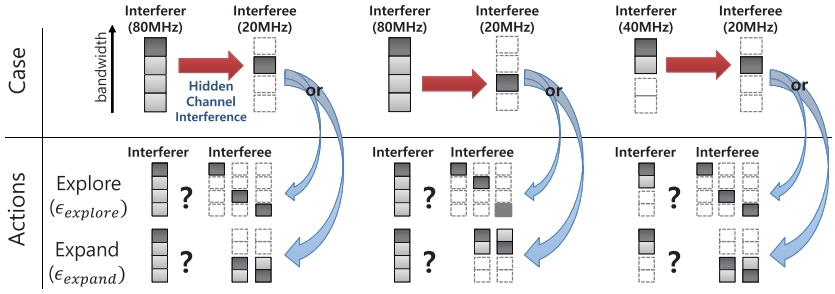

(a) 20MHz interferee

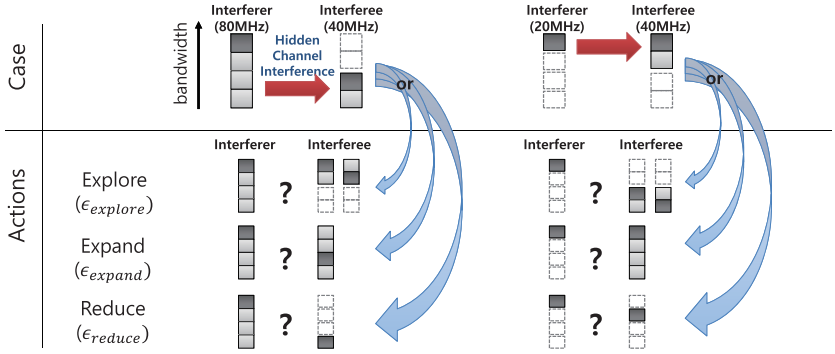

(b) 40MHz interferee

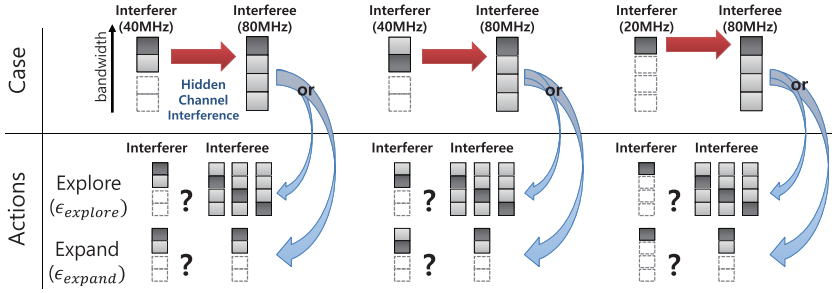

(c) 80MHz interferee

Figure 4.6: Action case studies according to bandwidth.

question marks represent possible specific channel switching options on each action type. These case studies assume that there is a gap between the primary and secondary CCA sensitivities, so they include expansion options in 20MHz and 40MHz cases,[2] where the location of each primary channel matters.

Our algorithm first determines which action type to be taken randomly. Then, within each type, a specific channel switch is also selected randomly. In doing so, the algorithm uses information from the post-CCA operation on each channel that the interferee previously occupied. If not used before, spectral and spatial reservations do not hold those channels, and thus the result of 'busy' from the post-CCA does not imply hidden channel collision.

There are many options in each action type that the interferee can take. The probability of selecting each action type is shown in the figure with ϵ. ϵ^{bw}_{expand}, ϵ^{bw}_{reduce} and $\epsilon^{bw}_{explore}$ represent the probabilities of taking expanding, reducing and exploring actions, respectively, on bandwidth bw. The choice of an action depends on which hidden collision has happened, and the summation of the probabilities for all the possible actions including 'stay' must be one. Primary channel location within an action is selected with uniform distribution among viable locations.

Defined actions with conditions are summarized in Algorithm 1. In each case of detected hidden channel collision, one or more possible

[2]The other case, without any gap, can be incorporated by setting the probability for expanding action to zero.

Algorithm 1 Pseudo code for PoBA

Precondition: After finishing a transmission
Input: Post-CCA results & ACK

if Entire bandwidth busy & no ACK **then**
  State: Entire hidden channel collision
  switch (Bandwidth)
  case 20MHz or 40MHz**:**
    Do *explore* or *stay* (or *expand* if possible) randomly
  case 80MHz**:**
    Do *explore* or *stay* randomly
else if Partial bandwidth busy & no ACK **then**
  State: Partial hidden channel collision
  switch (Bandwidth)
  case 40MHz**:**
    Do *reduce* or *explore* randomly
  case 80MHz**:**
    Do *reduce*
else
  State: No hidden channel collision
  switch (Bandwidth)
  case 20MHz**:**
    Do *expand* if possible with a small probability
  case 40MHz**:**
    Do *expand* if possible with a small probability
  case 80MHz**:**
    Do nothing
end if

actions can be chosen. In such cases, the algorithm randomly selects one with predefined probabilities as explained above. Even when a collision is not detected and current bandwidth is either 20MHz or 40MHz, expanding to 40MHz or 80MHz, respectively, is performed with predefined perturbation probability.

To maximize the performance of the bandwidth adaptation algorithm, we need to optimize the probabilities used in the algorithm. For example, detecting hidden channel collision on 40MHz bandwidth gives three possible actions. Depending on network condition, some of the actions alleviate the problem while some cause another hidden channel problem. It is impossible to know the result in advance from the perspective of the interferee because the information is limited[3]. Our approach is to try one of the possible solutions, and if it does not solve the problem, then try others in a greedy manner.

A natural question is whether the algorithm converges, and if so, whether it converges to the optimum. We find that in a dense network, it is impossible to guarantee convergence. For instance, if there are multiple interferers, one for each channel configuration that an interferee can have, the interferee will ping-pong among the possible options. Finding the network conditions that guarantee the convergence and optimality is an open research issue, which we leave for future work. However, using PoBA reduces packet error caused by the hidden channel problem, thus improving throughput. We show

[3]The uncertainty of the result is represented with the questions marks in Fig. 4.6

the PoBA's performance improvement via simulation.

4.4 Simulation Results

We implemented a simulator for *PoBA* — post-CCA and bandwidth adaptation — with C++.[4] The performance in terms of packet error rate, throughput, channel utilization and throughput fairness are measured with and without PoBA when closed loop channel estimation (i.e., explicit channel feedback) is applied. Also, to see the effect of the AMC, a simple AMC rule is used along with the post-CCA based bandwidth adaptation in the case of open loop (i.e., no explicit channel feedback) systems. The simple AMC scheme decreases one MCS level when a packet error is detected and increases one level if n_{succ} consecutive transmissions are successful, where we set $n_{succ} = 20$. Channel utilization is the bandwidth–time product used for successful packet transmissions over the entire available bandwidth.

The slot time, DIFS, PIFS, and SIFS are set to $9, 34, 25$, and $16\mu s$, respectively, and the transmission power is fixed at 17dBm. We assume that inter-transmission-attempt-time is $100\mu s$ and packet length is 1500bytes. The transmission time depends on the selected MCS level and the number of control messages (RTS, CTS and ACK)

[4]None of the available simulators (NS2, NS3, etc.) so far implements the 802.11ac contention mechanism in multi-channel environments. So, we implemented it with C++ in the same way as NS2/3 implements the simulator (event-queue based 'event driven simulator').

with the PLCP (Physical Layer Convergence Protocol) overhead of $20\mu s$.

The difference of the bandwidths that the interferee and the interferer are exploiting is considered so that the error rates of all the 20MHz channels are averaged to obtain effective PER (Packer Error Ratio). Then, the effective SINR of entire channel can be derived in an opposite way. The way of calculating effective PER and SINR is the same as in [24]. When calculating PER from SINR, we adopt the PER equation in [20] that counts various MAC-layer operations, such as MCS levels, Viterbi algorithm, and packet size.

The perturbation probability, ϵ_{per}^{bw}, is set to 0.05 for all bandwidths in the algorithm. The other ϵs, probabilities for choosing each action of *explore*, *expand* and *stay*, are 0.4, 0.4 and 0.2, respectively, for 20MHz hidden channel collision. They are 0.4, 0.4, 0.2 for the entire 40MHz hidden collision. When a partial hidden collision is detected on the 40MHz channel, the probabilities for *reduce*, *explore* and *stay* are 0.4, 0.4 and 0.2, respectively. Finally, the probabilities are 0.5 and 0.5 for *explore* and *stay*, respectively, in case of entire 80MHz hidden collision, while they are the same for *reduce* and *stay* in a partial 80MHz collision.

4.4.1 Case for a Chain Topology with Six APs

Fig. 4.7 illustrates a six transmitter–receiver chain topology for a simple demonstration of the effect of PoBA on performance, where APs

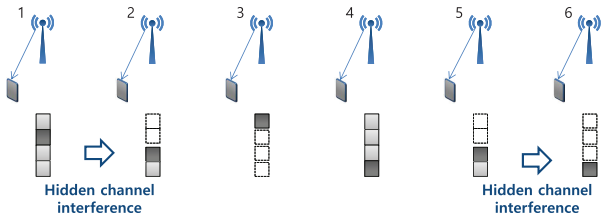

Figure 4.7: 6-chain topology for simple simulation.

Table 4.2: Simulation results for the toy topology in terms of error rate (%), throughput (Mbps), and channel utilization (%)

	Node	1	**2**	3	4	5	**6**
w/o PoBA	Err.	0.21	**86.93**	0.06	0.33	3.87	**69.41**
	Thr.	28.48	**0.31**	19.96	18.24	16.70	**1.43**
(closed)	Util.	34.88	**0.66**	54.71	22.34	35.22	**3.92**
w/ PoBA	Err.	0.27	**1.64**	1.50	0.07	3.12	**0.36**
	Thr.	21.78	**10.06**	15.80	18.08	16.75	**19.87**
(closed)	Util.	26.68	**20.15**	43.44	22.15	35.32	**54.48**
w/o PoBA	Err.	4.28	**3.95**	3.34	5.13	3.34	**3.82**
w/ AMC	Thr.	25.75	**8.75**	16.68	13.64	13.88	**4.86**
(open)	Util.	35.13	**67.78**	58.17	20.30	44.41	**77.65**
w/ PoBA	Err.	4.04	**2.96**	3.34	4.09	3.25	**3.31**
w/ AMC	Thr.	20.78	**11.99**	16.99	14.08	12.49	**15.79**
(open)	Util.	27.30	**36.01**	58.42	20.59	45.44	**59.30**

are transmitters and handsets are receivers. Depending on the distance among neighbors and channel configurations, some AP–handset pairs suffer the hidden channel problem. The distance and the initial channel configurations are set so that APs 2 and 6 suffer the HC problem due to APs 1 and 5.

The simulation results for the six chain topology are shown in Table. 4.2. In both closed and open loop systems, PoBA improves the throughput of APs 2 and 6. In closed systems, the algorithm improves the channel utilization and decreases the packet error rate. However, in open loop systems, error rates are already low even without PoBA because AMC adapts the MCS level to combat the bad channel condition. So, the channel utilization is high initially. In this case, PoBA leads interferee APs to raise their MCS levels by avoiding the hidden channel collision, which results in improved throughput even when the channel utilization decreases.

4.4.2 Case for Various Sized Random Networks

In the following simulation, random topologies with a fixed number of links are generated within a 100m $\times$ 100m grid. Each simulation is run for 5 sec, which is sufficient for the algorithm to asymptotically converge to a sub-optimal point if it exists, and each topology with the number of links is randomly generated 60 times. The results of the repeated simulations are averaged.

Fig. 4.8 and Fig. 4.9 shows the results. The density of the network

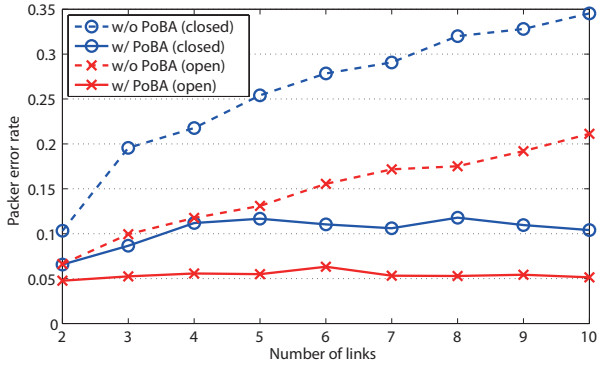

(a) Packet error rate

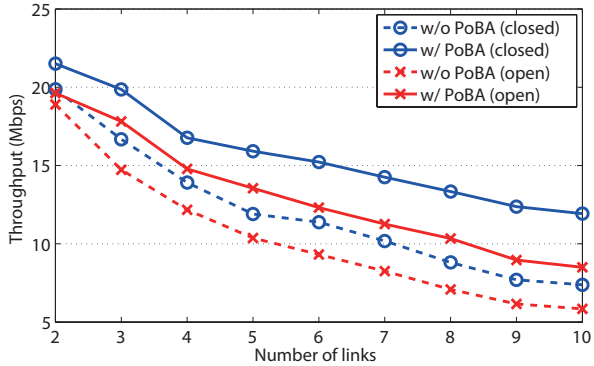

(b) Throughput

Figure 4.8: Simulation results with random topologies - error rate and throughput.

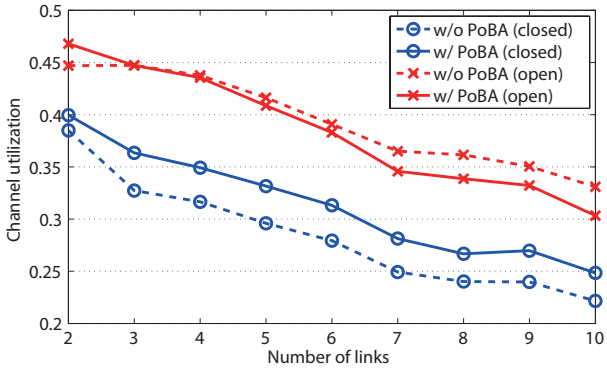

(a) Channel utilization

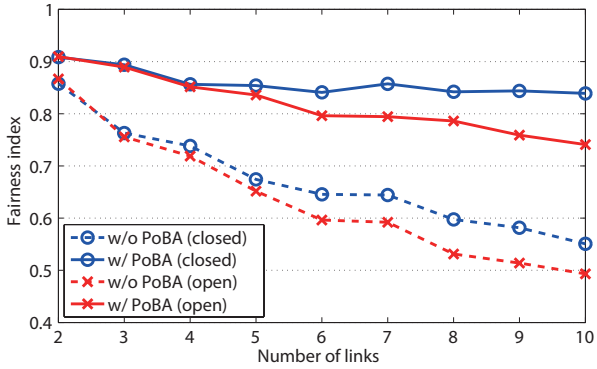

(b) Fairness

Figure 4.9: Simulation results with random topologies - utilization and fairness.

increases with the number of links in the grid. When the number of links is 10, in most dense networks, packet error rates without PoBA are around 35% and 22% in closed and open loop systems, respectively, as in Fig. 4.8(a). The error rates decrease by 25 and 17 percentage points, respectively, when PoBA is applied. These results lead to the increment of throughput per link as in Fig. 4.8(b). We can achieve 170% and 150% of throughput enhancement with PoBA in the closed and open systems, respectively.

The results of channel utilization show different tendencies in open and closed loop systems. In closed loop systems, the utilization increases, while decreasing in open loop systems. These results come from the fact that the AMC scheme tries to make use of the wireless bandwidth as much as possible by sacrificing throughput. So, bandwidth adaptation does not affect channel utilization a lot in open loop systems.

Finally, fairness performance increases by 0.25 point for both the closed and open loop systems. It reflects the fact that alleviating the hidden channel problem increases throughput of the nodes suffering the hidden channel collision all the time.

Performance in terms of error rate, throughput, utilization and fairness is achieved with PoBA even though the probabilities, ϵs, are not optimized. We leave the optimization for future work.

4.5 Summary

In this chapter, we firstly explored the effect of the bandwidth selection, then proposed post-CCA and PoBA which changes the bandwidth of each link dynamically and in a distributed manner to avoid the hidden channel problem. The post-CCA operation is a simple yet effective operation that enhanced the channel assessment capability and the PoBA exploits it. Using simulation we show that the PoBA enhances the throughput, fairness and utilization performance as well as decreases the packet error probability of a network.

The solution proposed in this chapter is a practical solution for its simplicity and applicability. Besides solving the hidden channel problem presented in this dissertation, we expect there are many applicable research areas such as distributed scheduling or more efficient contention mechanism that the solution can be used. In that sense, the post-CCA and PoBA are novel solutions.

Chapter 5

Conclusion

5.1 Research Contributions

In this dissertation, we presented the *hidden channel* (HC) problem that arises from use of heterogeneous bandwidths in the upcoming gigabit local area networks. This problem shows that the conventional CSMA/CA fails to achieve its goal in some network scenarios. We first illustrated the problem with an 802.11ac network as a reference system.

The HC problem occurs due to the heterogeneity of devices using different bandwidths. Also, the fixed transmission power results in different power density, which affects channel sensing/reserving ranges. Therefore we analyzed the HC problem scenario in the first part of this dissertation to understand the impact of CSMA contention parameter variations on asymmetric channel sensing/reserving behav-

iors. Through simulations, we confirmed the validity of our analytical model. The contention window sizes of an invader and a victim along with the packet transmission time of the victim mainly affect the performance with respect to collision probability and fairness. Under different scenarios, we observed that the performance of the victim fluctuates heavily while that of the invader is stable. This leads to the performance asymmetry between an invader and a victim, in terms of collision probability, fairness and stability.

In the next part of the dissertation, we formulated a centralized channel assignment problem with graph coloring and proposed a low complexity heuristic algorithm, *PCA*, as a first solution to the hidden channel problem. The objective of the assignment algorithm is to maximize the channel utilization while alleviating the HC problem. Simulation results indicate that the heuristic algorithm shows improved performance with respect to error rate, throughput and fairness when compared to the random and RSSI based allocation schemes. The impact of the enhanced RTS/CTS scheme on the performance is also evaluated. We then showed that solving the HC problem results in improved error rate and throughput of stations experiencing poor performance.

Because the *PCA* assumes that the bandwidth of each link is fixed by some reasons, it does not change the bandwidth. In order to expand the solution to an environment in which the bandwidth can be dynamically modified, we then explore the effect of the bandwidth se-

lection in the last part of the dissertation. Also, we performed simple experiments to show that the problem is real and to prove the validity of the our next solution, *PoBA*.

The post-CCA operation, another channel assessing stage after finishing a packet transmission, is suggested to alleviate the problem. The post-CCA helps mimic the CSMA/CD mechanism in the wired Ethernet to enhance the channel assessing capability. The results from the post-CCA operation can be used to dynamically adapt the bandwidth of each system in a distributed manner. The *PoBA* helps avoid the hidden channel problem in general network topologies. Thus, the algorithm increases the network throughput, channel utilization and fairness performance, and decrease the packet error rate.

5.2 Future Research Directions

The results of this dissertation can be applied in next-generation WLAN systems, such as 802.11ac and 802.11ax, to improve user experiences. Since both these systems will adopt OFDMA (Orthogonal Frequency Division Multiple Access), the entire bandwidth can be partially used according to the network conditions. So, the network-wide channel allocation (PCA alorithm) the CSMA/CD-like operation (post-CCA and PoBA) will be helpful. We leave the design for more system-specific operations for future work.

The hidden channel problem holds on the assumptions based on

the 802.11ac standard's parameters. The next versions of the wireless local area networks can have more flexible parameters, thus under certain conditions, the hidden channel problem may not arise. However, it is for sure that the next generation wireless local area networks will have heterogeneous bandwidths in the same frequency band, so it is expected that more problems related to the bandwidth will be encountered in such an environment.

Therefore, our future agenda is to explore the upcoming wireless local area systems and to find out other bandwidth related problems that will arise in the future heterogeneous bandwidth networks.

Bibliography

[1] National Instrument. [Online].
Available: http://www.ni.com/sdr/usrp

[2] WARP Project. [Online].
Available: http://www.warpproject.org

[3] GnuRadio. [Online]. Available: http://gnuradio.org

[4] Maxim intergrated, MAX2828/MAX2829 Single-/Dual-band 802.11a/b/g world-band tranceiver ICs. [Online]. Available: http://datasheets.maximintegrated.com/en/ds/MAX2828-MAX2829.pdf

[5] Qualcomm Inc. (Oct. 2013). The 1000x Data Challenge. [Online]. Available: http://www.qualcomm.com/solutions/wireless-networks/technologies/1000x-data

[6] Ericsson. (Jun. 2013). 5G Radio Access-Research and Vision. [Online]. Available: http://www.ericsson.com/res/docs/whitepapers/wp-5g.pdf

[7] Cisco. (Feb. 2012). Cisco visual networking index: Global mobile data traffic forecast update, 2011-2016. [Online]. Available: http://www.cisco.com

[8] *HEW SG March 2014 Closing Report*, IEEE SG report, [online]. Available: http://www.ieee802.org/ 11/Reports/hew_update.htm

[9] *Enhancements for Very High Throughput Operation in Bands below 6GHz*, IEEE standard amendment 802.11ac, 2011.

[10] *Enhancement for Higher Throughput*, IEEE standard amendment 802.11n, 2009.

[11] S. Jang and S. Bahk, "A channel allocation algorithm for reducing the channel sensing/reserving asymmetry in 802.11ac metworks," *IEEE Transactions on Mobile Computing,* vol. 14, no. 1, pp. 458-472, Mar. 2015.

[12] L. Deek, E. Garcia-Villegas, E. Belding, S.-J. Lee and K. Almeroth, "Intelligent channel bonding in 802.11n WLANs," *IEEE Transactions on Mobile Computing,* vol. 13, no. 6, pp. 1242-1255, Jun. 2014.

[13] E. Chai, Kang G. Shin, J. Lee, S.-J. Lee and R. H. Etkin, "Fast Spectrum Shaping for Next-Generation Wireless Networks," *IEEE Transactios on Mobile Computing,* vol. 13, no. 1, pp. 20-34, Jan. 2014.

[14] S. Yun, D. Kim and L. Qiu, "Fine-grained spectrum adaptation in WiFi networks," in *Proc. ACM MobiCom,* pp. 327-338, 2013.

[15] K. Chintalapudi, B. Radunovic, V. Balan and M. Buettner, "WiFi-NC: WiFi over narrow channels," in *Proc. ACM 9th USENIX Conf. NSDI,* 2012, p. 4.

[16] X. Zhang and Kang G. Shin, "Adaptive subcarrier nulling: Enabling partial spectrum sharing in wireless LANs," in *Proc. IEEE ICNP,* 2011, pp. 311-320.

[17] M. X. Gong, B. Hart, L. Xia and R. Want, "Channel Bounding and MAC protection mechanisms for 802.11ac," in *Proc. IEEE Globecom,* 2011, pp. 1-5.

[18] M. Park, "IEEE 802.11ac: Dynamic bandwidth channel access," in *Proc. IEEE ICC,* 2011, pp. 1-5.

[19] E. Perahia and M. X. Gong, "Gigabit wireless LANs: An overview of IEEE 802.11ac and 802.11ad," *ACM SIGMOBILE,* vol. 15, pp. 23-33, 2011.

[20] D. Qiao, S. Choi and K. G. Shin, "Goodput analysis and link adaptation for IEEE 802.11a wireless LANs," *IEEE Transactions on Mobile Computing,* vol. 1, no. 4, pp. 278-202, Oct. 2002.

[21] D.-J. Deng, K.-C. Chen and R.-S. Cheng, "IEEE 802.11ax: Next generation wireless local area networks," on *Proc. IEEE QShine,* 2014, pp. 77-82.

[22] T. A. Levanen, J. Pirskanen, T. Koskela, J. Talvitie and M. Valkama, "Radio interface evolution towards 5G and enhanced local area communications," *IEEE Access,* vol. 2, pp. 1005-1029, Sep. 2014.

[23] A. Al-Dulaimi, S. Al-Rubaye, Q. Ni and E. Sousa, "5G communication race: Pursuit of more Capacity Triggers LTE in unlicensed band," *IEEE Vehicular Technology Magazine,* vol. 10, no. 1, pp. 43-51, Mar. 2015.

[24] D. Halperin, W. Hu, A. Sheth and D. Wetherall, "Predictable 802.11 Packet Delivery from Wireless Channel Measurements," *ACM SIGCOMM,* 2010.

[25] J. Gross and J. Yellen, *Graph Theory and its Applications*. Boca Raton, FL, USA: CRC Press, 1998, pp. 323-362.

[26] A. Mishra, S. Banerjee and W. Arbaugh, "Weighted Coloring based Channel Assignment for WLANs," *ACM SIGMOBILE,* vol. 9, pp. 19-31, 2005.

[27] A. Mishra, V. Shrivastava, D. Agarwal, S. Banerjee and S. Ganguly, "Distributed Channel Management in Uncoordintated Wireless Environment," *ACM MobiCom,* pp. 170-181, 2006.

[28] A. Mishra, V. Brik, S. Banerjee, A. Srinivasan and W. Arbaugh, "A Client-driven Approach for Channel Management in Wireless LANs," in textitProc. IEEE Infocom, pp. 1-12, 2006.

[29] S. Abbas and S. Hong, "A Scheduling and Synchronization Technique for RAPIEnet Switches Using Edge-Coloring of Conflict Multigraphs," textitJournal of Communications and Networks vol. 15, pp. 321-328, 2013.

[30] L. Jiang and J. Walrand, "A Distributed CSMA Algorithm for Throughput and Utility Maximization in Wireless Networks," *IEEE/ACM Transactions on Networking,* vol. 18, no. 3, pp. 960-972, Jun. 2010.

[31] J. Ni, B. (R.) Tan and R. Srikant, "Q-CSMA: Queue-Length-Based CSMA/CA Algorithms for Achieving Maximum Throughput and Low Delay in Wireless Networks," *IEEE/ACM Transactions on Networking,* vol. 20, no. 3, pp. 825-836, Jun. 2012.

[32] K. Kim , K. Kwak and B. Choi, "Performance Analysis of Opportunistic Spectrum Access Protocol for Multi-Channel Cognitive Radio Networks," *Journal of Communications and Networks,* vol. 15, pp. 77-86, 2013.

[33] Y. Choi, S. Park and S. Bahk, "Multichannel Random Access in OFDMA Wireless Networks," *IEEE Journal on Selected Areas in Communications,* vol. 24, no. 3, pp. 603-613, Mar. 2006.

[34] J. Choi and S. Bahk, "Cell Throughput Analysis of the Proportional Fair Scheduler in the Single Cell Environment," *IEEE*

Transactions on Vehicular Technology, vol. 56, no. 2, pp. 766-778, Mar. 2007.

[35] L. Kiaer and K. Yellen, "Weighted Graphs and University Course Timetabling," *Elsivier Computers Ops. Res.,* vol. 19, no.'1, pp. 59-67, 1992.

[36] D. Werra, "An Introduction to Timetabling," *Elsivier European Journal of Operational Research,* vol. 19, pp. 151-162, 1985.

[37] T. Müller, "Constraint based Timetabling," Ph.D. dissertation, Faculty of Mathematics and Physics, Charles University in Prague, Praha, Czech Republic, 2005.

[38] J. Lee, W. Kim, S. Lee, D. Jo, J. Ryu, T. Kwon and Y. Choi, "An Experimental Study on the Capture Effect in 802.11a Networks," in *Proc. 2nd ACM International Workshop on Wireless Network Testbeds, Experimental Evaluation and Characterization,* pp. 19-26, 2007.

[39] R. Jain, D. Chiu, and W. Hawe, "A Quantitative Measure Of Fairness And Discrimination For Resource Allocation In Shared Computer Systems," Tech. Rep. TR-301, DEC Res., Palo Alto, CA, USA, Sep. 1984.